CLEARINGHOUSE FOR FEDERAL SCIENTIFIC AND TECHNICAL INFORMATION, CFSTI
DOCUMENT MANAGEMENT BRANCH 410.11

LIMITATIONS IN REPRODUCTION QUALITY

Accession # AD 606262

☑ 1. We regret that legibility of this document is in part unsatisfactory. Reproduction has been made from best available copy.

☐ 2. A portion of the original document contains fine detail which may make reading of photocopy difficult.

☐ 3. The original document contains color, but distribution copies are available in black-and-white reproduction only.

☐ 4. The initial distribution copies contain color which will be shown in black-and-white when it is necessary to reprint.

☐ 5. Limited supply on hand; when exhausted, document will be available in Microfiche only.

☐ 6. Limited supply on hand; when exhausted document will not be available.

☐ 7. Document is available in Microfiche only.

☐ 8. Document available on loan from CFSTI (TT documents only).

☐ 9.

Processor: eah

NBS___ 9/64

A SIMPLE RELATIONSHIP BETWEEN THE SHOCK AND EXPANSION PRESSURE COEFFICIENTS AS A BASIS FOR STUDYING TWO-DIMENSIONAL HYPERSONIC FLOW

J. L. Raymond*

P-1011

January 15, 1957

* Aeronautics Department, The RAND Corporation

The RAND Corporation
1700 MAIN ST. • SANTA MONICA • CALIFORNIA

ABSTRACT

A simple relation between the two-dimensional wedge pressure coefficients for shock and expansion is shown to apply for the entire hypersonic regime. As a consequence, the hypersonic small-disturbance theory expressions for these coefficients are further simplified as are calculations of pressure distributions on arbitrary two-dimensional configurations at hypersonic speeds.

SUMMARY

Over the range of hypersonic similarity parameter $0.2 \leq K \leq \infty$, the reduced pressure coefficients for compression and expansion have been observed[1] to have very nearly the relationship

$$\bar{C}_{p_c} + \bar{C}_{p_e} = \gamma+1 \qquad (1)$$

where $\bar{C}_{p_c}$ and $\bar{C}_{p_e}$ are calculated results of two-dimensional hypersonic small-disturbance theory.[1][2] It is demonstrated that for $K \geq 1.4$

$$\bar{C}_{p_c} \cong \gamma+1 + \frac{2}{\gamma K^2} \qquad (2)$$

and

$$\bar{C}_{p_e} \cong -\frac{2}{\gamma K^2} \qquad (3)$$

These reduced pressure coefficients give substantially the same force coefficients for simple convex airfoil shapes as those given by either two-dimensional hypersonic small-disturbance theory or by shock-expansion theory. Their use permits considerable savings in computation time in calculating force coefficients for two-dimensional airfoils. Agreement with limited test data is good.

CONTENTS

ABSTRACT ii

SUMMARY iii

LIST OF FIGURES v

SYMBOLS AND NOMENCLATURE vi

Section

I INTRODUCTION 1

II. DISCUSSION 2

III. TWO-DIMENSIONAL HYPERSONIC SMALL-DISTURBANCE THEORY 4

IV. COMPARISON BETWEEN ISENTROPIC AND SHOCK COMPRESSION 5

V. REGION OF VALIDITY OF ISENTROPIC FLOW 11

VI. CHANGE OF SIMILARITY PARAMETER THROUGH A SHOCK OR AN EXPANSION 14

VII. APPROXIMATE PRESSURE COEFFICIENTS 17

VIII. PRESSURE DISTRIBUTION OVER A CONVEX AIRFOIL 19

IX. RESULTS 24

X. CONCLUSIONS 26

Appendix: AN APPLICATION OF PISTON FLOW TO TWO-DIMENSIONAL HYPERSONIC FLOW 27

REFERENCES 33

LIST OF FIGURES

Fig.	Title
1.	Two-Dimensional Pressure Coefficients
2.	The Normalized Sum of Two-Dimensional Pressure Coefficients
3.	Schematic of an Oblique-Shock
4a.	Air Properties for Isentropic and Oblique-Shock Compressions
4b.	Velocity and Mach Number for Isentropic and Oblique-Shock Compressions
5.	A Region of Small-Angle Isentropic Flow
6.	The Variation of Similarity Parameter Through a Compression and an Expansion
7.	Force Coefficients for a Flat Plate
8.	A Comparison of Normal Force Coefficients for a Flat Plate
9.	Schematic of an Airfoil at Angle of Attack
10.	A Comparison of Experimental Lift Coefficient with Theory
11.	A Comparison of Experimental Drag Coefficient with Theory
12.	Lift Coefficient for a Modified Half-Wedge Airfoil
13.	Drag Coefficient for a Modified Half-Wedge Airfoil
14.	Schematic of an Advancing Piston
15.	Schematic of a Retreating Piston

SYMBOLS AND NOMENCLATURE

a	speed of sound
C_p	force coefficient
$\bar{C}_p$	C_p/δ^2
c	chord
C_D	D/qc
$\bar{C}_D$	C_D/δ^3
C_L	L/qc
$\bar{C}_L$	C_L/δ^2
C_M	M/qc
$\bar{C}_M$	C_M/δ^2
C_p	$\frac{p-p_\infty}{q}$
$\bar{C}_p$	$\frac{C_p}{\delta^2}$
c_v	specific heat at constant volume
c_p	specific heat at constant pressure
D	drag per unit span
H	$\frac{1}{M^2\delta^2}$
K	$M\delta$, hypersonic similarity parameter
L	lift per unit span
M	Mach number
N	normal force per unit span
O	of the order of
p	static pressure

q	dynamic pressure
T	temperature
t	time
u	speed in the x direction
V	air speed
x,y,z	wing coordinates

Greek Symbols

α	angle of attack
Γ	$\frac{\gamma-1}{2}$
γ	ratio of specific heats, c_p/c_v, 1.4 in this paper
δ	local slope, radians
θ	wave angle, radians

Subscripts

∞	free stream
c	compression
e	expansion
F	following
l	lower surface
n	normal to the surface
o	stagnation
P	piston
u	upper surface
w	shock wave

I. INTRODUCTION

The pressure coefficients for two-dimensional flow over the hypersonic regime $0.5 \leq K \leq \infty$ have been derived by various authors[1,2,3] based on the ideas of hypersonic small-disturbance theory. The application of these coefficients to specific two-dimensional airfoils has been made for $K \leq 1.0$ by Dorrance[4] for essentially isentropic flows and by Linnell[3] for $0.1 \leq K \leq 10$.

The present paper introduces approximations for pressure coefficients which in general are within two percent of shock-expansion or 'exact' two-dimensional hypersonic small-disturbance values. The present equations are simple; in addition an expression relating the hypersonic similarity parameter K before and after an expansion is derived and some remarks on the corresponding compression relationship are made. The result is a simplified practical way of calculating the forces on two-dimensional airfoils over the entire range of speeds represented by $0.5 \leq K \leq \infty$ within the framework of the two-dimensional hypersonic small-disturbance theory.

An analysis of the compression phenomenon for the isentropic expansion and comparison with oblique shock compression is made. An investigation into the flow phenomenon as to why $\bar{C}_{p_c} + \bar{C}_{p_e} = \gamma+1$ is made. The relationship between several theories is brought out together with the present calculations.

The derivation of the forces on two-dimensional flat plate by use of the piston analogy is made. The results agree well with those of two-dimensional hypersonic small-disturbance theory, for $K \geq 2.0$, approximately.

II. DISCUSSION

To bring out the deviations of $\bar{C}_{p_c} + \bar{C}_{p_e}$ from the sum $\gamma+1$, it is pertinent to study either the derivatives of each coefficient and compare their variation with K, or to examine the derivatives of the sum.* The latter approach is made here.

For $K \leq 1.0$ the flow is isentropic for compression as well as expansion. This has been established by Busemann[5] to the second order and by Dorrance[4] to the first order in δ and is shown in Fig. 1. Both theoretical treatments follow.

Including the second order in flow deflection, Busemann gives

$$C_{p_c} = C_1 \delta + C_2 \delta^2 \tag{4a}$$

and

$$C_{p_e} = - C_1 \delta + C_2 \delta^2 \tag{4b}$$

from which

$$\bar{C}_{p_c} + \bar{C}_{p_e} = 2 C_2 \tag{5}$$

where[5]

$$C_1 = \frac{2}{\sqrt{M_\infty^2 - 1}}$$

and

$$C_2 = \frac{(M_\infty^2 - 2)^2 + \gamma M_\infty^4}{2(M_\infty^2 - 1)^2}$$

---

* This suggestion is acknowledged with thanks to Dr. W. D. Hayes, Associate Professor of Aero. Eng., Princeton University.

Hence the derivative is

$$\frac{d}{dK_\infty}\left(\bar{C}_{p_c} + \bar{C}_{p_e}\right) = \frac{4}{(M_\infty^2-1)^2}\left[(1+\gamma)M_\infty^3 - 2M_\infty\right] - \frac{4M_\infty}{(M_\infty^2-1)^3}\left[(1+\gamma)M_\infty^4 - 2M_\infty^2 + 1\right] \tag{6}$$

where $M_\infty = K_\infty/\delta$, which is valid[5] for $\delta_{max} < \delta < 5^\circ$, $1.3 < M_\infty < 15$ or essentially for $K_\infty \leq 1.0$ (also see Fig. 1). It is always negative, increasing positively toward zero, so that as $M_\infty \to \infty$, it is zero. Laitone[5] has tabulated C_2 (or b_2 of Ref. 9, Table 3) over the range of Mach number $1.1 \leq M_\infty \leq 100$. However, since the flow is postulated as isentropic, the deflection angle must be kept small enough so that $K_\infty < 1.0$ approximately. Figure 2 shows the effect of δ on the variation of $2C_2$ with K_∞. It must be noted that the effect of δ is rather pronounced but the values of $2C_2$ are nonetheless in agreement with the other curves shown. (Further remarks on validity will subsequently follow.) The preceding indicates that provided $K_\infty = O(1)$, the Mach number can increase indefinitely and still provide reasonable agreement with other pertinent isentropic theories.

Dorrance has shown [Ref. 4, Eq. (29)], that for essentially isentropic flows, $K_\infty \leq 1.0$, $M_\infty > 3.19$, that

$$\bar{C}_{p_c} = \frac{2}{K_\infty} + \frac{\gamma+1}{2} + \frac{\gamma+1}{6}K_\infty \tag{7}$$

and

$$\bar{C}_{p_e} = -\frac{2}{K_\infty} + \frac{\gamma+1}{2} - \frac{\gamma+1}{6}K_\infty \tag{8}$$

From which $\bar{C}_{p_c} + \bar{C}_{p_e} = \gamma+1$ and $\frac{d}{dK_\infty}\left(\bar{C}_{p_c} + \bar{C}_{p_e}\right) = 0$. This result is indicated in Fig. 2.

III. TWO-DIMENSIONAL HYPERSONIC SMALL-DISTURBANCE THEORY

A similar analysis based on the results of hypersonic small-disturbance theory[1][2] can be made. The results are valid for $0.5 \leq K \leq \infty$ and hence complement and extend the isentropic treatment. The equations are

$$\bar{C}_{p_c} = \frac{\gamma+1}{2} + \sqrt{\left(\frac{\gamma+1}{2}\right)^2 + \frac{4}{K^2}} \qquad (9)$$

for oblique shocks and

$$\left.\begin{aligned} \bar{C}_{p_e} &= \frac{2}{\gamma K^2}\left[\left(1 - \frac{\gamma-1}{2}K\right)^{\frac{2\gamma}{\gamma-1}} - 1\right] && K \leq \frac{2}{\gamma-1} \\ \text{or} \\ \bar{C}_{p_e} &= -\frac{2}{\gamma K^2} && K \geq \frac{2}{\gamma-1} \end{aligned}\right\} \qquad (10)$$

for isentropic expansion. The derivative is negative for $K < 0.4$, becomes positive for $0.4 \leq K < 2.35$ and then negative once again for $2.35 \leq K \leq \infty$. However, unlike the Busemann approximation which depends upon β, the greatest difference between $\bar{C}_{p_c} + \bar{C}_{p_e}$ and $\gamma+1$ is about .6 percent at $K = 2.35$ over the range $0.2 \leq K \leq \infty$ (Fig. 2).

IV. COMPARISON BETWEEN ISENTROPIC AND SHOCK COMPRESSION

To gain an insight as to the phenomenon $\bar{C}_{p_c} + \bar{C}_{p_e} = \gamma+1$, it was thought worthwhile* investigating the isentropic compression in the region $.2 \leq K \leq \infty$ and comparing with the oblique shock compression, Eq. (3).

Results take on the form of pressure, density, temperature, Mach number and velocity variations with K_∞ and comparing them.

The isentropic compression coefficient is by definition

$$\bar{C}_{p_c} = \frac{2}{\gamma M_\infty^2} \left[\left\{ \frac{1 + \frac{\gamma-1}{2} M_\infty^2}{1 + \frac{\gamma-1}{2} M^2} \right\}^{\frac{\gamma}{\gamma-1}} - 1 \right] \tag{11}$$

From Eq. (32) (which follows) we have $\frac{1}{K} = \frac{1}{K_\infty} + \frac{\gamma-1}{2}$ from which

$$K = \frac{K_\infty}{1 + \frac{\gamma-1}{2} K_\infty} \tag{12}$$

Putting Eq. (12) into Eq. (11) and dividing by δ^2 gives

$$\bar{C}_{p_c} = \frac{2}{\gamma K_\infty^2} \left[\left\{ \frac{\delta^2 + \frac{\gamma-1}{2} K_\infty^2}{\delta^2 + \frac{\frac{\gamma-1}{2} K_\infty^2}{(1 + \frac{\gamma-1}{2} K_\infty)^2}} \right\}^{\frac{\gamma}{\gamma-1}} - 1 \right] \tag{13}$$

It is interesting to deviate briefly and note that for $\delta << 1$

---

* This suggestion was made by Dr. C. Gazley, Jr., Aerodynamicist, The RAND Corporation, and is acknowledged with thanks.

$$\bar{C}_{p_c} = \frac{2}{\gamma K_\infty^2}\left[\left(1 + \frac{\gamma-1}{2} K_\infty\right)^{\frac{2\gamma}{\gamma-1}} - 1\right] \qquad (14)$$

Equation (14) is reasonably good even to K_∞ as small as unity where it is about 10 percent high as compared to the value given by Eq. (13) with δ = .1 radians and agrees even better with Eq. (9) for $K_\infty < 1.0$ (Fig. 1). It is to be noted from Eq. (14) that

$$\left(\frac{p}{p_\infty}\right)_c = \left(1 + \frac{\gamma-1}{2} K_\infty\right)^{\frac{2\gamma}{\gamma-1}} \qquad (15)$$

which is similar in form to

$$\left(\frac{p}{p_\infty}\right)_e = \left(1 - \frac{\gamma-1}{2} K_\infty\right)^{\frac{2\gamma}{\gamma-1}} \qquad K_\infty \leq \frac{2}{\gamma-1} \qquad (16)$$

$$= 0 \qquad K_\infty \geq \frac{2}{\gamma-1}$$

the result obtained for isentropic expansion by Cole [Ref. 2, Eq. (6-16)]. In fact, if compressive and expansive flows are designated by positive and negative K_∞ (4)(10)* (corresponding respectively to positive or negative slope, $\pm\delta$), Eq. (15) represents both compression and expansion, respectively.

The reduced pressure coefficient based on Eqs. (2), (3), (4), (7), (8), (9), (10), (13) and (14) are plotted in Fig. 1.

We proceed with comparison of pressure, temperature, density and velocity ratios based on both isentropic and oblique shock compressions. The remaining isentropic gas properties were calculated from Eq. (15) by using

---

* It can easily be shown that Lighthill's Eq. (4)(10) and Eq. (15) are identical, though not the same in appearance.

$$\frac{p}{p_\infty} = \left(\frac{\rho}{\rho_\infty}\right)^\gamma = \left(\frac{T}{T_\infty}\right)^{\frac{\gamma}{\gamma-1}} \tag{17}$$

The velocity ratio can be calculated by use of the energy equation, together with the static temperature ratio obtained from Eq. (17). The energy equation is

$$\frac{V^2}{2} + C_p T = \frac{V_\infty^2}{2} + C_p T_\infty \tag{18}$$

Rearranging we get

$$\left(\frac{V}{V_\infty}\right)^2 = 1 - \frac{2 C_p T_\infty}{V_\infty^2}\left(\frac{T}{T_\infty} - 1\right)$$

from which

$$\frac{V}{V_\infty} = \sqrt{1 - \frac{2\delta^2}{(\gamma-1)K_\infty^2}\left(\frac{T}{T_\infty} - 1\right)} \tag{19}$$

It is interesting to calculate Eq. (19) in the hypersonic small-disturbance limit

$$\frac{V}{V_\infty} = \sqrt{1 - \frac{2\delta^2}{(\gamma-1)K_\infty^2}\left\{\left[\frac{\delta^2 + \frac{\gamma-1}{2}K_\infty^2}{\delta^2 + \frac{\frac{\gamma-1}{2}K_\infty^2}{1 + \frac{\gamma-1}{2}K_\infty}^2}\right] - 1\right\}}$$

For $K_\infty > 1$, $\delta \ll 1$,

$$\frac{V}{V_\infty} = \sqrt{1 - \left(\frac{\gamma-1}{2}\right)\delta^2} \tag{19a}$$

The oblique-shock properties are now calculated. From Eq. (9)

$$\frac{p}{p_\infty} = 1 + \frac{\gamma K_\infty^2}{2}\left[\frac{\gamma+1}{2} + \sqrt{\left(\frac{\gamma+1}{2}\right)^2 + \left(\frac{2}{K_\infty}\right)^2}\right] \tag{20}$$

By the Rankine-Hugoniot relationship, the density ratio is

$$\frac{\rho}{\rho_\infty} = \frac{1 + \frac{\gamma+1}{\gamma-1}\frac{p}{p_\infty}}{\frac{\gamma+1}{\gamma-1} + \frac{p}{p_\infty}} \tag{21}$$

and by the equation of state we get the shock temperature ratio

$$\frac{T}{T_\infty} = \left(\frac{p}{p_\infty}\right)\left(\frac{\rho_\infty}{\rho}\right) \tag{22}$$

For the velocity ratio we see (from Fig. 3)

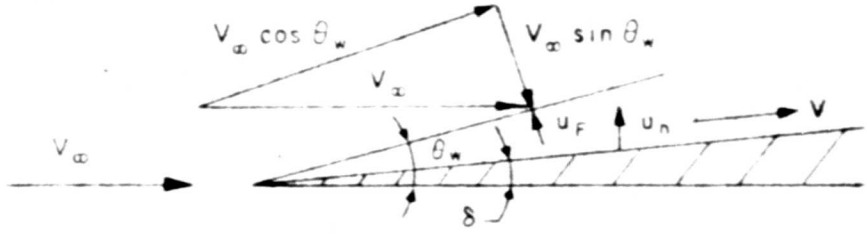

Figure 3

that the velocity V after the shock is

$$V^2 = V_\infty^2 \cos^2\theta_w + (V_\infty \sin\theta_w - u_F)^2 \tag{23}$$

where u_F, the perturbation velocity following the shock wave, is related to the normal velocity u_n produced by the slope δ, by

$$u_p = \frac{u_n}{\cos(\theta_w - \delta)} = \frac{V_\infty \delta}{\cos(\theta_w - \delta)} \tag{24}$$

Substituting Eq. (24) into Eq. (23) we have

$$V^2 = V_\infty^2 \cos^2 \theta_w + V_\infty^2 \sin^2 \theta_w - 2V_\infty^2 \delta \frac{\sin \theta_w}{\cos(\theta_w - \delta)} + \frac{V_\infty^2 \delta^2}{\cos^2(\theta_w - \delta)}$$

Hence

$$\frac{V^2}{V_\infty^2} = 1 - 2\delta\theta_w + \delta^2 \tag{25}$$

assuming small angles δ and θ_w. From Eq. (9) we have

$$\bar{C}_{p_c} = 2\frac{\theta_w}{\delta} = \bar{C}_{p_c}(\gamma, K) \tag{9}$$

so that

$$\frac{V}{V_\infty} = \sqrt{1 - \delta^2(\bar{C}_{p_c} - 1)} \tag{26}$$

$$\frac{V}{V_\infty} = \sqrt{1 - \gamma\delta^2} \tag{26a}$$

limit $K \to \infty$

Equation (26a) is quite similar in form to Eq. (13a). The relations expressed by Eqs. (15), (17), (19), (20), (21), (22), and (26) are plotted in Figs. 4a and 5b.

From Fig. 4a the pressure rise in isentropic flow is greater than that for oblique shock compression previously noted by Laitone[5]

for $K > 1.4$. It is noted that for $K \leq 1.3$, there is no large difference in pressure ratio for either type of compression, a phenomenon noted by many writers.[4][5] Since p/p_∞ due to shock compression is proportional to K^2, Eq. (20), then as $K \to \infty$, $\bar{C}_{p_c}$ tends to a finite limit. On the other hand, non-viscous theory shows that the isentropic pressure ratio (Eq. (15)) is proportional to K^7 as $K \to \infty$, hence $\bar{C}_{p_c}$ tends to infinity. The temperature and velocity ratios indicate the nature of the dissipative shock flow when compared to the respective isentropic relations. The temperature rise is higher for oblique shock waves than for isentropic flow. The velocity decrease is small[9] for small flow deflections characteristic of the small-disturbance oblique shocks considered and even less for isentropic flow. It should be noted that for convenience, K is generally used for K_∞ although strictly speaking, the latter is the free-stream similarity parameter.

V. REGION OF VALIDITY OF ISENTROPIC FLOW

The regime of Mach number-deflection angle over which shock flow can be assumed to be isentropic is investigated below (although this has been done from slightly different viewpoints previously[4][5]). From Fig. 1, it is evident that for $K \leq 1.0$, the limiting isentropic compression coefficient, Eq. (14), (for $\delta = 0^\circ$) and the shock coefficient, Eq. (9), are substantially the same. Since $K_\infty = M_\infty \delta$, and since the two-dimensional hypersonic small-disturbance theory is valid for $\delta \leq 1$ say $\delta \leq 0.2$, several important deductions can be made. The first is that $\bar{C}_{p_c} = \frac{2\theta_v}{\delta} \geq 3.5$ for isentropic compression (at $K = 1.0$). The corresponding Mach number normal to the shock is $M \sin \theta_v \approx M \theta_v = K \frac{\theta_v}{\delta}$ from which $M \theta_v = 1.75$ (and decreases with decreasing K).

The above observations result in Fig. 5. The upper small-disturbance limit for δ is taken as 0.2 radians, while the lower limit is $\delta = 0$. The left-hand limit is for shock attachment while the right-hand limit becomes $\delta \to 0$ as $M \to \infty$.

An important feature of the flow mentioned briefly above, is that isentropic compression results in less compression than shock compression below $K \leq 1.0$ approximately, for $\delta > 0$ (depending on the magnitude of δ), although the reverse is true for $K \geq 1.0$ (Fig. 4a). It is seen that the greater the flow deviation in isentropic compressive flow, the less the compression. Laitone[5] in comparing approximate solutions of oblique shock and isentropic compression indicates this K effect in a different way. That is, for small flow

deflections and for $M_\infty > 1.82$, isentropic compression produces greater pressure increases than the oblique shock wave even for very small deflection angles. However, for $M_\infty > 2.4$, the oblique shock wave produces a much smaller pressure increase than isentropic compression, even for very large flow deviations.

The value of Fig. 5 is brought out in Fig. 1, by observing Busemann's results. That is, in order to establish the validity of Busemann's results in the $\bar{C}_p$ - K plane, an example calculation, $\delta = 0.10$, and 0.01, was taken. Here it is seen that for $K \leq 1.0$, the results of this theory do not differ greatly from the others shown, in fact, agrees to within 6.3 percent of the isentropic compression value of Eq. (13) for $\delta = 0.10$ at $K = 1.0$, and hence is closely related to other theories. It must be noted that the Busemann result varies somewhat with flow deviation selected, although only for $K < 0.5$. For example, for $\delta = 0.10$ the compression and expansion coefficients are higher than those for $\delta = 0.01$ by 16 percent and 14 percent at $K = 0.20$ but these differences decrease until for $K > 0.50$ they are negligible. The agreement between Busemann's results for $\delta = .01$ and the other isentropic results at $K = 0.20$ is excellent. It appears, then, that for a selected K, Busemann's solution agrees better with other theories as $\delta \to 0$, even though $M \to \infty$. This surprising result leads one to believe that the small-perturbation effect is perhaps more dominant than the Mach number effect, at least in this case. Figure 5 indicates the Mach number-deflection angle relationship graphically for isentropic flow, for $K = 1.0$.

It is noted that Eq. (13) provides a new solution for the regime of

$K > 1$, as well as fitting into the previous theories for $K \leq 1.0$. Obviously, Eq. (13) does not break down at high K and is seen to go beyond the bounds of Fig. 5 (for example the solution for $\delta = 0.10$ for $K > 1.0$).

VI. CHANGE OF SIMILARITY PARAMETER THROUGH A SHOCK OR AN EXPANSION

It has been previously pointed out[4] that for essentially isentropic flow where $K \leq 1.0$, $M \geq 3.19$, that pressure coefficients can be calculated and integrated over two-dimensional airfoils to obtain force coefficients without regard to the number and type of wave fronts preceding the local slope (see Ref. 4, Eq. (29)). Because of isentropy, it is possible to calculate free-stream pressure coefficients as a function of K_∞ based on M_∞ and local slope which in turn makes possible the closed form solutions for various shaped airfoils. This technique is used in getting force coefficients in linear two-dimensional flows and has been known for some time.[6]

However, for $K > \frac{4}{\gamma+1}$, the flow is characterized by strong shocks and it is no longer possible to disregard the shock fronts, consequently it has not been possible to relate the local pressure coefficient directly to free-stream conditions in closed form. It was necessary, therefore, to find the local similarity parameter based on local slope and local Mach number in order to calculate local pressure ratios through a wave front. These ratios can be related to free-stream static pressure by a consecutive series of multiplications of the local pressure ratios at any downstream position progressing systematically upstream until free-stream conditions are reached. A closed form solution is derived in Sec. VIII which applies to convex airfoils.

The relationship for the change in K through an oblique shock has been calculated (Ref. 2, Eq. (8-27)). It is useful in the development which follows in Sec. VIII.

$$\frac{H}{H_\infty} = 1 + \frac{\gamma-1}{2} \frac{1}{H_\infty} \left[\bar{C}_{p_c}(H_\alpha) - 1 \right] \qquad (27a)$$

or

$$\left(\frac{M_\infty}{M}\right)^2 = 1 + \frac{\gamma-1}{2} K_\infty^2 \left[\bar{C}_{p_c}(K_\infty) - 1\right] \qquad (27b)$$

where $\bar{C}_{p_c}(K_\infty)$ is given by Eq. (9).

The direct relationship however, between similarity parameter before and after an isentropic expansion through the angle δ is derived below. The ratio of local static pressure ratio through an expansion [from Ref. 6, Eq. (3.9)] is

$$\frac{p}{p_\infty} = \left[\frac{1 + \frac{\gamma-1}{2} K_\infty^2}{1 + \frac{\gamma-1}{2} K^2}\right]^{\frac{\gamma}{\gamma-1}} \qquad (28)$$

From Ref. 2, Eq. (5-17), for $K_\infty = O(1)$

$$\frac{p}{p_\infty} = \left(1 - \frac{\gamma-1}{2} K_\infty\right)^{\frac{2\gamma}{\gamma-1}} \qquad (29)$$

Equating Eqs. (28) and (29) results in

$$\left[\frac{\delta^2 + \frac{\gamma-1}{2} K_\infty^2}{\delta^2 + \frac{\gamma-1}{2} K^2}\right]^{\frac{\gamma}{\gamma-1}} = \left(1 - \frac{\gamma-1}{2} K_\infty\right)^{\frac{2\gamma}{\gamma-1}} \qquad (30)$$

from which

$$\frac{1}{K} = \frac{1 - \frac{(\gamma-1)}{2} K_\infty}{K_\infty \sqrt{2\frac{\delta^2}{K_\infty} + \left(1 - \frac{\gamma-1}{2}\delta^2\right)}} \qquad (31)$$

For $\delta << 1$, the final equation becomes

$$\frac{1}{K} = \frac{1}{K_\infty} - \frac{\gamma-1}{2} \quad , \qquad \frac{1}{K_\infty} = \frac{\gamma-1}{2} \qquad (31a)$$

Using Eqs. (28) and (15) the similar expression for compression is

$$\frac{1}{K} = \frac{1 + \left(\frac{\gamma-1}{2}\right) K_\infty}{K_\infty \sqrt{\left(1 - \frac{\gamma-1}{2} \delta^2\right) - 2 \frac{\delta^2}{K_\infty}}} \qquad (32)$$

which for $K_\infty > 1$ and $\delta \to 0$ becomes

$$\frac{1}{K} = \frac{1}{K_\infty} + \frac{\gamma-1}{2} \qquad (32a)$$

Equation (32) is seen to agree very well with Eq. (27) for $\delta \to 0$, $K < 1.0$ (Fig. 6). It must be noted that Eqs. (31a) and (32a) are mirror images of each other about the line $\frac{1}{K} = \frac{1}{K_\infty}$. It is instructive to note the limit values of $\frac{1}{K}$ as $\frac{1}{K_\infty}$ approaches its minimum value. For compression, as $K_\infty \to \infty$, (i.e. $\sqrt{H_\infty} \to 0$) K remains finite due to the fact that Mach number decreases through a shock or in isentropic compression. On the other hand, for the expansion process at $K_\infty = 5.0$, the resulting $K = \infty$. Physically, then, the flow will expand to $M = \infty$ when $K_\infty = 5.0$ at the beginning of an expansion, because the local temperature, hence, the speed of sound goes to zero.

Another relationship for the change in similarity parameter through a shock is derived in Sec. VIII. It is based on Eqs. (2) and (27b) and is considerably simpler in form.

VII. APPROXIMATE PRESSURE COEFFICIENTS

Approximate expressions for pressure coefficient can be derived from Eq. (9) by expanding into series which converge for both $K \geq \frac{4}{\gamma+1}$. The radical in Eq. (9) can be written

$$\sqrt{\left(\frac{\gamma+1}{2}\right)^2 + \frac{4}{K^2}} = \frac{2}{K}\sqrt{1 + \left(\frac{\gamma K}{2}\right)^2} \qquad (34)$$

which converges for $K < \frac{4}{\gamma+1}$.

Expanding the radical on the right-hand side into a series results in

$$\sqrt{1 + \left(\frac{\gamma K}{2}\right)^2} = 1 + \frac{(\gamma K)^2}{2^3} - \frac{(\gamma K)^4}{2^7} + O\left[\frac{(\gamma K)^6}{2^9}\right] \qquad (34)$$

Hence the approximate expression for Eq. (9) becomes

$$\bar{C}_{p_c} = \left(\frac{\gamma+1}{2}\right)^{\gamma} + \frac{2}{K} + \frac{(\gamma-1)^2 K}{4}, \qquad K < \frac{4}{\gamma+1} \qquad (35)$$

and by use of Eqs. (1) and (35),

$$\bar{C}_{p_c} = \left(\frac{\gamma+1}{2}\right)^{\gamma} - \frac{2}{K} - \frac{(\gamma-1)^2 K}{4} \qquad (36)$$

Equations (35) and (36) are quite similar to Eqs. (7) and (8) (see Figs. 7 and 8). The procedure is the same for obtaining $\bar{C}_{p_c}$ in the region $K > \frac{4}{\gamma+1}$ and results in

$$\frac{\bar{C}_{p_c}}{\gamma+1} = 1 + \frac{1}{(\gamma K)^2} - \frac{1}{(\gamma K)^4} + O\left[\frac{2}{(\gamma K)^6}\right], \qquad (37)$$

and

$$\frac{\bar{C}_{p_e}}{\gamma+1} = -\frac{1}{(\Gamma K)^2} + \frac{1}{(\Gamma K)^4} \qquad \frac{1}{\gamma+1} < K \leq \frac{1}{\Gamma}\sqrt{\frac{\gamma}{\gamma-\Gamma}} \qquad (38)$$

$$= -\frac{2}{\gamma K^2} \qquad K > \frac{1}{\Gamma}\sqrt{\frac{\gamma}{\gamma-\Gamma}}$$

It can be shown that $\bar{C}_{p_e}$ calculated by Eq. (38) is equal to that for total vacuum for $K = \frac{1}{\Gamma}\sqrt{\frac{\gamma}{\gamma-\Gamma}}$, and is less for K greater than this value. This is not physically possible. In this case, the $\bar{C}_{p_e}$ was taken as equal to $-\frac{2}{\gamma K^2}$ which corresponds to $p_e = 0$. From an engineering viewpoint, there is no practical difference essentially in force coefficients calculated by Eqs. (37) and (38) and those by 'exact' small-disturbance theory, Eqs. (9) and (10). Examples of force coefficients calculated by Eqs. (2), (3), (35), (36), (37) and (38) will follow (Figs. 7, 8, 10, 11, 12 and 13).

VIII. PRESSURE DISTRIBUTION OVER A CONVEX AIRFOIL

As mentioned in Sec. VI, a closed form solution for convex airfoils will be derived using present results. For $K > 1$ there will be a strong attached shock on either or both sides of a thin airfoil in supersonic flow. Thus a method of relating the local pressure, p, to the free-stream pressure p_∞, is needed to compute the aerodynamic coefficients. Only the normal force coefficient is treated here, it being typical. Other coefficients can be similarly calculated. A selected airfoil of arbitrary convex shape at angle of attack is shown in Fig. 9.

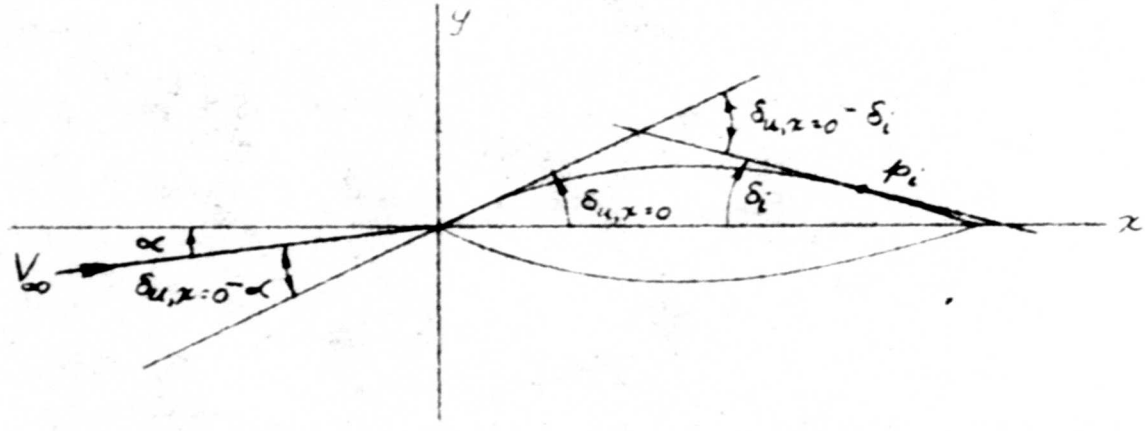

Figure 9 - Schematic of an Airfoil at Angle of Attack

The following treats the selected case of a strong shock followed by an isentropic expansion (on one side of the airfoil). Using Eq. (2) results in

$$\frac{p}{p_\infty} = 1 + \frac{\gamma K_\infty^2 \bar{C}_{p_c}}{2}$$

$$= 2 + \frac{\gamma(\gamma+1)K_\infty^2}{2} \quad , \qquad K_\infty > 1.4 \qquad (39)$$

From Eq. (16) we have for isentropic expansion

$$\frac{p}{p_\infty} = \left(1 - \frac{(\gamma-1)}{2} K_\infty\right)^{\frac{2\gamma}{\gamma-1}} \qquad K_\infty < \frac{2}{\gamma-1}$$

$$= 0 \qquad K_\infty \geq \frac{2}{\gamma-1} \tag{16}$$

Using Eq. (27b) we get for the similarity parameter ratio through a shock

$$\left(\frac{K_\infty}{K}\right)^2 = 1 + \frac{\gamma-1}{2} K_\infty^2 \left[\bar{C}_{p_c}(K_\infty) - 1\right] \tag{27b}$$

which is simplified by substituting Eq. (2). Solving for K we get

$$K = \sqrt{\frac{2\gamma}{\gamma^2(\gamma-1) + \frac{2(2\gamma-1)}{K_\infty^2}}} \tag{40}$$

The result of Eq. (40) is plotted in Fig. 6.

It must be noted that the characteristic angle (for K_∞) in Eq. (40) is based on the initial angle between leading-edge slope and free-stream. This angle differs, in general, for the upper and lower surfaces and is respectively,

$$\delta_{u,\infty} = \left|\delta_{u,x=0} - \alpha\right|$$

and

$$\delta_{\ell,\infty} = \left|-\delta_{\ell,x=0} + \alpha\right| \tag{41}$$

Now Eq. (16) is applicable in the isentropic region after the shock. In notation of the ratio of the pressure at the i^{th} point to that immediately behind the shock

$$\frac{p_i}{p} = 1 - \frac{\gamma-1}{2} M \left| \delta_i - \delta_{x=0} \right|^{\frac{2\gamma}{\gamma-1}} \tag{42}$$

The ratio of the pressure p_i at i^{th} point to that immediately behind the shock p is expressed in terms of the known quantities M after the shock and the net change in slope or net turning angle. The Mach number M immediately after the shock is readily calculated by dividing Eq. (40) by Eqs. (41) for the upper and lower surfaces, respectively. By consecutive multiplication

$$\frac{p_i}{p_\infty} = \left(\frac{p_i}{p} \right) \left(\frac{p}{p_\infty} \right) \tag{43}$$

Therefore, by substitution into Eq. (43) there results finally

$$\frac{p_i}{p_\infty} = \left[1 - \frac{(\gamma-1)\left| \delta_i - \delta_{x=0} \right|}{2\delta_{x=0}} \sqrt{\frac{2\gamma}{\gamma^2(\gamma-1) + \frac{3(2\gamma-1)}{K_{\infty_{x=0}}^2}}} \right]^{\frac{2\gamma}{\gamma-1}} \left[\frac{\gamma(\gamma+1)}{2} K_{\infty_{x=0}} + 2 \right] \tag{44}$$

It must be noted that δ_i is the only variable with chordwise position for either surface. The normal force coefficient is

$$C_N = \frac{2}{c\gamma M_\infty^2 \alpha^2} \int_0^c \frac{p_l - p_u}{p_\infty} \, dx \tag{45}$$

Hence $\bar{C}_N$ can be calculated by substituting Eq. (44) (applied to upper and lower surfaces) into Eq. (45). Explicitly

$$\bar{C}_N = \frac{2}{c\gamma M_\infty^2 \alpha^2} \int_0^c \left[1 - \frac{(\gamma-1)(\delta_{\ell,1} - \delta_{\ell,x=0})}{2\delta_{\ell,x=0}} \sqrt{\frac{2\gamma}{\gamma^2(\gamma-1) + \frac{2(\gamma-1)}{K^2_{\infty,\ell,x=0}}}} \right]^{\frac{2\gamma}{\gamma-1}} \left[2 + \frac{\gamma(\gamma+1)}{2} K^2_{\infty,\ell,x=0} \right] - \left[1 - \frac{(\gamma-1)(\delta_{u,x=0} - \delta_{u,1})}{2\delta_{u,x=0}} \sqrt{\frac{2\gamma}{\gamma^2(\gamma-1) + \frac{2(2\gamma-1)}{K^2_{\infty,u,x=0}}}} \right]^{\frac{2\gamma}{\gamma-1}} \left[2 + \frac{\gamma(\gamma+1)}{2} K^2_{\infty,u,x=0} \right] dx \qquad (46)$$

Equation (46) can be written as

$$\bar{C}_N = \int_0^c \left[A \left[1 - B(\delta_{\ell,1} - \delta_{\ell,x=0}) \right]^{\frac{2\gamma}{\gamma-1}} - C \left[1 - D(\delta_{u,x=0} - \delta_{u,1}) \right]^{\frac{2\gamma}{\gamma-1}} \right] dx \qquad (46a)$$

where the only variables are

$$\delta_{\ell,1} = \left(\frac{dy}{dx}\right)_{\ell,1} \quad \text{and} \quad \delta_{u,1} = \left(\frac{dy}{dx}\right)_{u,1} \qquad (47)$$

and all the other quantities, A, B, C, D, are fixed for a selected free-stream Mach number, angle of attack, profile and ratio of specific heats. For a symmetric airfoil about the chord line, local slopes at a given

chordwise station are related by

$$\delta_{\ell,1} = -\delta_{u,1}$$

For the case of no shock wave at the leading edge, Eq. (16) is directly applicable.

IX. RESULTS

The Flat Plate

The flat plate (where $K = M\alpha$) is especially easy to treat. In this case, the lift and drag can be calculated by the use of Eqs. (35) and (36) for $K < \frac{4}{\gamma+1}$, and by Eqs. (37) and (38) for $K > \frac{4}{\gamma+1}$. However, the case for $K \gtrsim 1.4$, results in an extremely simple expression for $\bar{C}_N$, namely from Eqs. (2) and (3) we get

$$\bar{C}_N = \bar{C}_{p_c} - \bar{C}_{p_e} = (\gamma + 1) + \frac{4}{\gamma K^2} \tag{49}$$

The results of Eq. (49) are plotted in Fig. (7) along with those of two-dimensional hypersonic small-disturbance theory, linear theory and the isentropic results from Eqs. (7), (8), (35), (36), (37) and (38).

It must be noted that in calculating $\bar{C}_N$ for a flat plate, for example, the expression for $\bar{C}_N$, Eq. (49) is the most practical to use ($K > 1.4$). The expression for pressure coefficients as expressed by Eqs. (2) and (3) are the simplest in practice and involve negligible error for $K > 1.4$, for all cases worked out herein.

It appears that the combination of Eqs. (2), (3), (35) and (36) achieve excellent agreement with other theories throughout the entire range of K. The simplicity of Eq. (49) along with the accuracy shown in Fig. 8 makes it useful to K as low as 1.4 and with less than 5 percent difference from the 'exact' Eqs. (9) and (10). It will be noted that

$$C_N = C_D \qquad (40)$$

for a flat plate, within the small-angle approximation.

A. Double Wedge

A comparison of theory and test is made in Figs. 10 and 11. Calculations using Eqs. (35) and (37) for $K = 1.4$ and Eqs. (2) and (3) for $K \geq 1.4$ are compared with those of shock-expansion theory and results of wind-tunnel tests on a double-wedge airfoil with an aspect ratio equal to one in the Langley 11-inch hypersonic wind tunnel. In general, the present method is in good agreement with shock-expansion theory, the error varying from 0 at $\alpha = 0°$ to 1.5 percent high at $\alpha = 24°$ for C_L. The same trend holds for C_D with the maximum error varying from 0 at $\alpha = 0$ to about one-half percent at $\alpha = 24°$.

The Modified Half Wedge

The present results are compared with the theory of Cole and Van Dyke as well as the shock-expansion theory for a modified half wedge for $M_\infty = 18$ in Figs. 12 and 13. The differences in the results are not thought significant, there being general agreement over the range of angle of attack shown.

IX. CONCLUSIONS

The following aspects of flow for $0.2 \leq K \leq \infty$ have been pointed out:

1. There is a unique relationship (11) between the reduced pressure coefficients $\bar{C}_{p_c} + \bar{C}_{p_e} = \gamma+1$ over the range $0.2 \leq K \leq \infty$.

2. The isentropic region of linear and second-order theories is a function of K and δ (Fig. 5). The Mach number can be much greater than one for isentropy.

3. The limiting case of isentropic compression $\delta = 0$, is a guide to the behavior of the oblique-shock phenomenon for $0.2 \leq K \leq \infty$, being nearly equal to oblique shock in nature for $K \leq 1.0$ and indicating the nature of an upper bound for reversible compressive flows for $K \geq 1.0$.

4. The use of Eqs. (2), (3), (35) and (36) are quite accurate for engineering calculations for surprisingly large flow deviations when compared to limited test data, as well as other theories, for $0.2 \leq K \leq \infty$.

Appendix

AN APPLICATION OF PISTON FLOW TO TWO-DIMENSIONAL HYPERSONIC FLOW

The flows in two adjacent planes parallel to each other and normal to the flight path (velocity vector) are essentially independent of each other, since it can be shown that at hypersonic speeds, the time for a sound wave to traverse the distance between these planes is large compared to the time for the wedge or body to pass through them, i.e. in the ratio $\frac{1}{M}$. The flow at any fixed plane (in space) appears almost independent of adjacent transverse planes and depends only upon the time history of the body as it passes by. Consequently, for a two-dimensional wing, a fixed observer sees the motion of a gas similar to that generated by a piston moving in a long tube.[8][9] The duration of piston motion is c/V_∞ and the vertical position of the 'piston' is a function of time.

The piston problem has been solved by J. D. Cole[2] and can be applied to two-dimensional hypersonic flows.

The following will be devoted to this application and will finally be compared with the results of two-dimensional hypersonic small-disturbance theory (Cole, Van Dyke). Figure 14 illustrates the shock phenomenon, simulated by a piston moving upward.

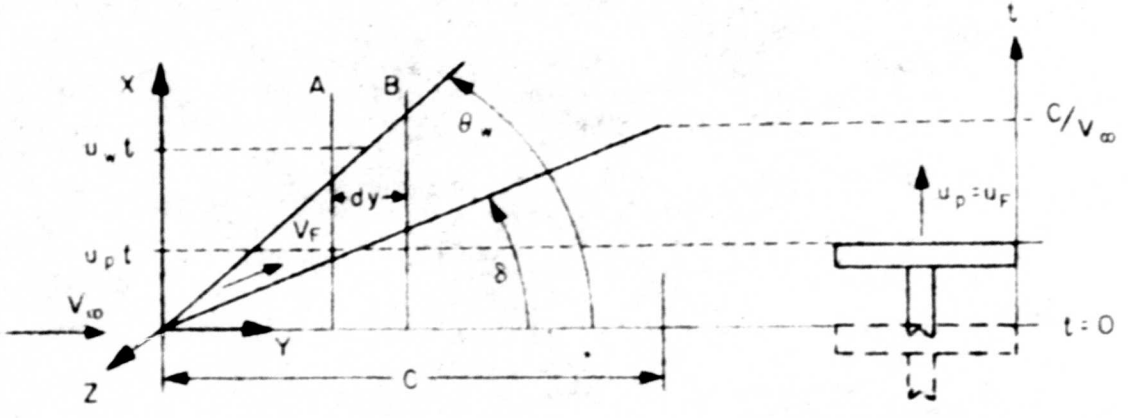

Fig. 14 A Two-Dimensional Compression

The mass above the piston is

$$\left(\frac{\rho}{\rho_\infty}\right) \rho_\infty \, dx \, dy \, dz \qquad \text{(I-1)}$$

The force of the piston on the air is

$$dF = \frac{d}{dt}\left(\frac{\rho}{\rho_\infty}\right) \rho_\infty \, dx \, dy \, dz \, u_p \qquad \text{(I-2)}$$

Since

$$dy = V_\infty \, dt \qquad \text{(I-3a)}$$

and

$$u_p = V_\infty \, \delta = u_p \qquad \text{(I-3b)}$$

by substituting Eqs. (I-3) into (I-2) and integrating,

$$F = \left(\frac{\rho}{\rho_\infty}\right) \rho_\infty \, V_\infty^2 \, \delta \, dz \int_{u_p t}^{u_w t} dx$$

$$= \frac{\rho}{\rho_\infty} (\rho_\infty) \, V_\infty^2 \, \delta \, dz (u_w - u_p) t \qquad \text{(I-4)}$$

From Ref. 2, Eq. (5-24),

$$u_w = \left(\frac{\gamma+1}{4}\right) u_p + \sqrt{\left(\frac{\gamma+1}{4}\right)^2 u_p^2 + a_\infty^2} \qquad \text{(I-5)}$$

and noting that

$$t = \frac{c}{V_\infty} , \qquad \text{(I-6)}$$

the total time of impulse, by substitution of Eqs. (I-5) and (I-6) into Eq. (I-4),

$$I = \left(\frac{\rho}{\rho_\infty}\right)\left(\frac{1}{2}\rho_\infty V_\infty^2\right) bc\, dz\, 2\left[\frac{(\gamma-3)}{4}\tau + \sqrt{\left(\frac{\gamma+1}{4}\right)^2 s^2 + \frac{1}{M_\infty^2}}\right] \tag{I-7}$$

From Eq. (20)

$$\frac{p}{p_\infty} = 1 + \frac{\gamma(\gamma+1)}{4}K^2 + \gamma K\sqrt{1+\left(\frac{\gamma+1}{4}\right)^2 K^2} \tag{I-8}$$

and from Rankine-Hugoniot shock theory, Eq. (21), we have

$$\frac{\rho}{\rho_\infty} = \frac{1+\left(\frac{\gamma+1}{\gamma-1}\right)\frac{p}{p_\infty}}{\frac{\gamma+1}{\gamma-1}+\frac{p}{p_\infty}} \tag{I-9}$$

Hence substituting Eq. (I-8) into (I-9) and then (I-9) into (I-7),

$$C_T = \frac{I}{\frac{1}{2}\rho_\infty V_\infty^2\, c\, dz\, \delta^2} = C_{N_c}$$

$$= 2\left[\left(\frac{\gamma-3}{4}\right)+\sqrt{\left(\frac{\gamma+1}{4}\right)^2+\frac{1}{K^2}}\right]\left[\frac{1+\frac{\gamma+1}{\gamma-1}\frac{p}{p_\infty}}{\frac{\gamma+1}{\gamma-1}+\frac{p}{p_\infty}}\right]$$

$$= 2\left[\left(\frac{\gamma-3}{4}\right)+\sqrt{\left(\frac{\gamma+1}{4}\right)^2+\frac{1}{K^2}}\right]$$

$$\left[\frac{1+\left(\frac{\gamma+1}{\gamma-1}\right)\left(1+\frac{\gamma(\gamma+1)}{4}K^2+\gamma K\sqrt{1+\left(\frac{\gamma+1}{4}\right)^2 K^2}\right)}{\frac{\gamma+1}{\gamma-1}+1+\frac{\gamma(\gamma+1)}{4}K^2+\gamma K\sqrt{1+\left(\frac{\gamma+1}{4}\right)^2 K^2}}\right] \tag{I-10}$$

It will be noted that

$$\lim_{K \to \infty} \bar{C}_p = \gamma+1 \qquad \text{(I-11)}$$

which is a well-known hypersonic result. Equation (I-10) expresses the force coefficient in hypersonic similarity form, of the piston on the gas; hence it is also the force of the gas on the piston and is a positive force for positive δ. Comparison with the results of hypersonic-small disturbance theory, Eq. (9), is deferred until later.

The following is the case for the withdrawing piston at constant speed, u_p, which simulates the expansion side of a two-dimensional flat plate. Figure 15 illustrates this situation.

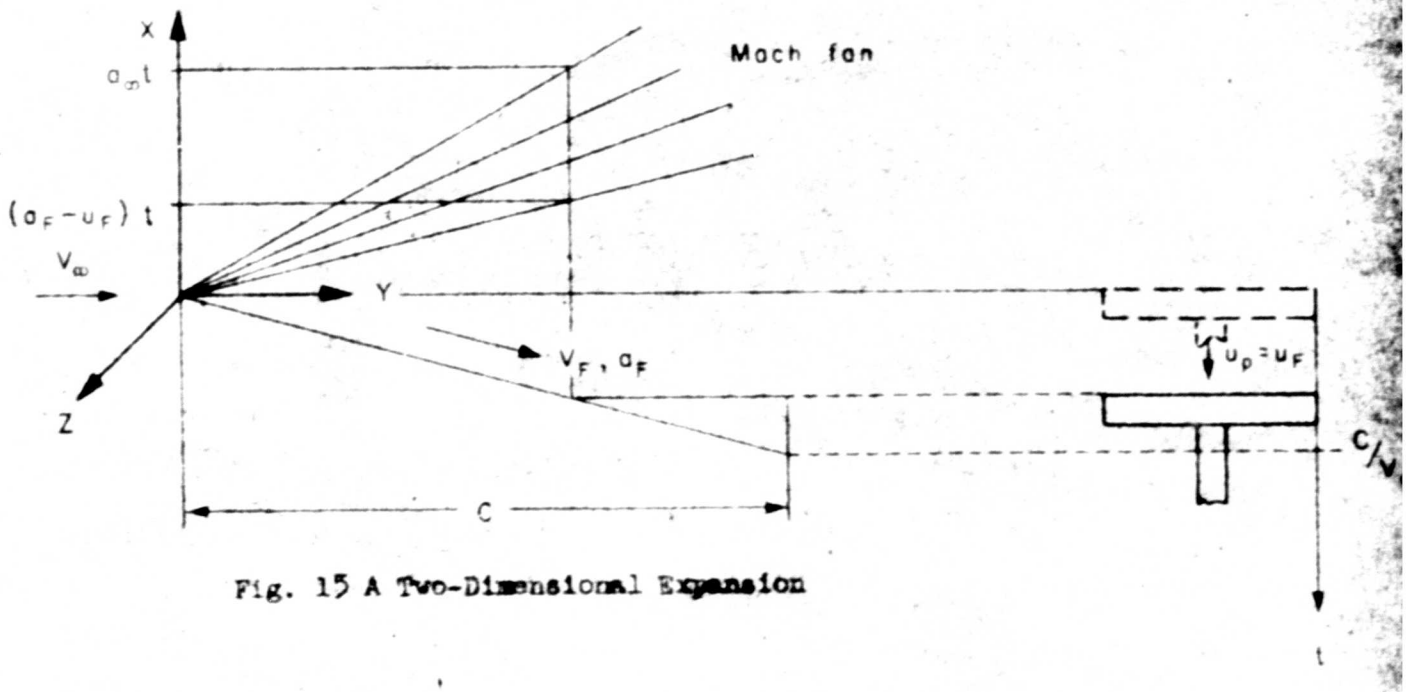

Fig. 15 A Two-Dimensional Expansion

In this case, both the velocity and the speed of sound along the x axis vary linearly[2] through the fan so that Eq. (I-2) upon integration becomes

$$F = \rho_\infty V_\infty \, dz \int_{(a_F - u_F)t}^{a_\infty t} \left(\frac{\rho}{\rho_\infty}\right) u \, dx \qquad \text{(I-12)}$$

Since this is an isentropic flow,

$$\frac{\rho}{\rho_\infty} = \left(\frac{a}{a_\infty}\right)^{\frac{2}{\gamma-1}} \tag{I-13}$$

and in the expansion fan [see Ref. 2, Eqs. (6-5a), and (6-5b)],

$$a = a_\infty + \frac{a_\infty t - x}{a_\infty t - (a_p - u_p)t}(a_p - a_\infty)$$

$$u = u_p \frac{a_\infty t - x}{a_\infty t - (a_p - u_p)t} \tag{I-14}$$

Noting that $u_p = u_p = -\delta V_\infty$ and substituting Eqs. (I-13) and (I-14) into Eq. (I-12), we get

$$F = -\frac{\rho_\infty V_\infty^2 \delta\, dz}{a_\infty^{\frac{2}{\gamma-1}}} \int_{(a_p-u_p)t}^{a_\infty t} \left[a_\infty + \frac{(a_\infty t - x)(a_p - a_\infty)}{a_\infty t - (a_p-u_p)t}\right]^{\frac{2}{\gamma-1}} \left[\frac{a_\infty t - x}{a_\infty t - (a_p-u_p)t}\right] dx \tag{I-15}$$

which when integrated becomes

$$F = \frac{-2\rho_\infty c\, a_\infty^2\, dz}{(\gamma-1)} \left\{\frac{(\gamma+1)}{2\gamma}\left[1 - \left(1 - \frac{\gamma-1}{2}K\right)^{\frac{2\gamma}{\gamma-1}}\right] - \left[1 - \left(1 - \frac{\gamma-1}{2}K\right)^{\frac{\gamma+1}{\gamma-1}}\right]\right\} \tag{I-16}$$

which is the force of the piston on the airflow through the expansion fan.

$$\bar{C}_p = \frac{4}{(\gamma-1)K^2}\left\{\left[1 - \left(1 - \frac{\gamma-1}{2}K\right)^{\frac{\gamma+1}{\gamma-1}}\right] - \frac{\gamma+1}{2\gamma}\left[1 - \left(1 - \frac{\gamma-1}{2}K\right)^{\frac{2\gamma}{\gamma-1}}\right]\right\} \quad K < \frac{2}{\gamma-1} \tag{I-17}$$

• For $K \geq \frac{2}{\gamma-1}$ it will be noted that Eq. (I-17) agrees exactly with Cole's result, Eq. (3).

$$\bar{C}_p = -\bar{C}_{p_e} = \frac{2}{\gamma K^2} = \bar{C}_{B_e} \qquad \text{(I-18)}$$

In summing up the present results of the piston application for compression, Eq. (I-10), and expansion, Eq. (I-17), it is seen that they compare favorably with hypersonic small-disturbance theory, except for the expansion case for $K \sim 2.0$. At $K = 1.0$ the present expansion result is 46 percent low while at $K = 2.0$ it is 14 percent low as compared with $-\bar{C}_{p_e}$ of Eq. (10). This taken to be an indication that at $K \sim 2.0$, the idea of independent flows in the transverse direction is being violated to an appreciable degree for expansive flows. The shock results of the piston, Eq. (I-10), agree very well with the small-disturbance result of Eq. (9), throughout the range $1.0 \leq K \leq \infty$.

It should be noted that the relations expressed by Eqs. (I-5) for u_w, and Eq. (I-8) for p/p_∞, can be evaluated by Eq. (2). The force coefficient for a piston in compression (corresponding to Eq. (I-10)) is then

$$\bar{C}_p = \left(\gamma - 1 + \frac{2}{K^2}\right) \left[\frac{1 + \frac{\gamma+1}{\gamma-1}\left(\frac{\gamma(\gamma+1)}{2} K^2 + 2\right)}{\frac{2\gamma-1}{\gamma-1} + \frac{\gamma(\gamma+1)}{2} K^2}\right] \qquad \text{(I-19)}$$

REFERENCES

1. Van Dyke, Milton D., A Study of Hypersonic Small-Disturbance Theory, NACA Report 1194, 1954.

2. Cole, J. D., C. Gazley, Jr., and B. P. Williams, 'Class Notes for an Hypersonic Aerodynamics Course,' UCLA Extension, Spring Term 1956 and 1957.

3. Linnell, Richard D., 'Two-Dimensional Airfoils in Hypersonic Flows,' J.A.S., Vol. 16, No. 1, January 1949, pp. 22-30.

4. Dorrance, William D., 'Two-Dimensional Airfoils at Moderate Hypersonic Velocities,' J.A.S., Vol. 19, No. 9, September 1952, pp. 593-600.

5. Laitone, Edmund V., Exact and Approximate Solutions of Two-Dimensional Oblique Shock Flow, J.A.S., Vol. 14, No. 1, January 1947, pp. 25-41.

6. Liepman, H. W., and A. E. Puckett, Introduction to the Aerodynamics of a Compressible Fluid, John Wiley and Sons, Inc., New York, 1947.

7. McLellan, Charles, H., Mitchel H. Bertram, and John A. Moore, An Investigation of Four Wings of Square Plan Form at a Mach Number of 6.86 in the Langley 11-Inch Hypersonic Tunnel, NACA RM L51D17, June 29, 1951.

8. Lees, Lester, Hypersonic Flow, Institute of Aeronautical Sciences Preprint No. 554, June 20-24, 1955.

9. Hayes, Wallace D., 'On Hypersonic Similitude,' Quar. Appl. Math., Vol. 5, No. 1, April 1947, pp. 105 - 106.

10. Lighthill, M. J., 'Oscillating Airfoils at High Mach Number,' J.A.S., Vol. 20, No. 6, June 1953, pp. 402-406.

11. Raymond, J. L., E. P. Williams, 'A Simple Relation Between the Shock and Expansion Pressure Coefficients for Two-Dimensional Hypersonic Flow,' J.A.S., Vol. 24, No. 5, May 1957 (to be published).

BLANK PAGE

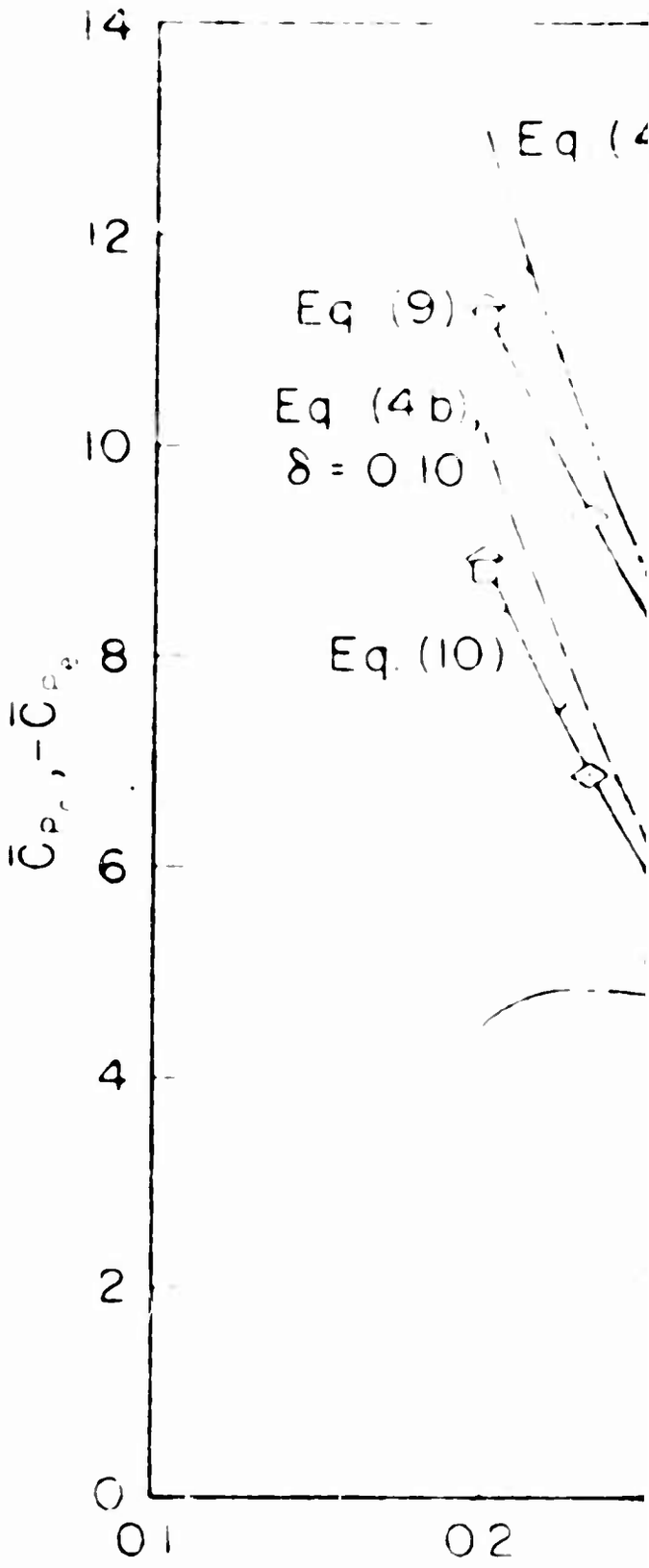
14
12
10
8
6
4
2
0
01
02
Eq (4
Eq (9)
Eq (4b)
δ = 0 10
Eq. (10)

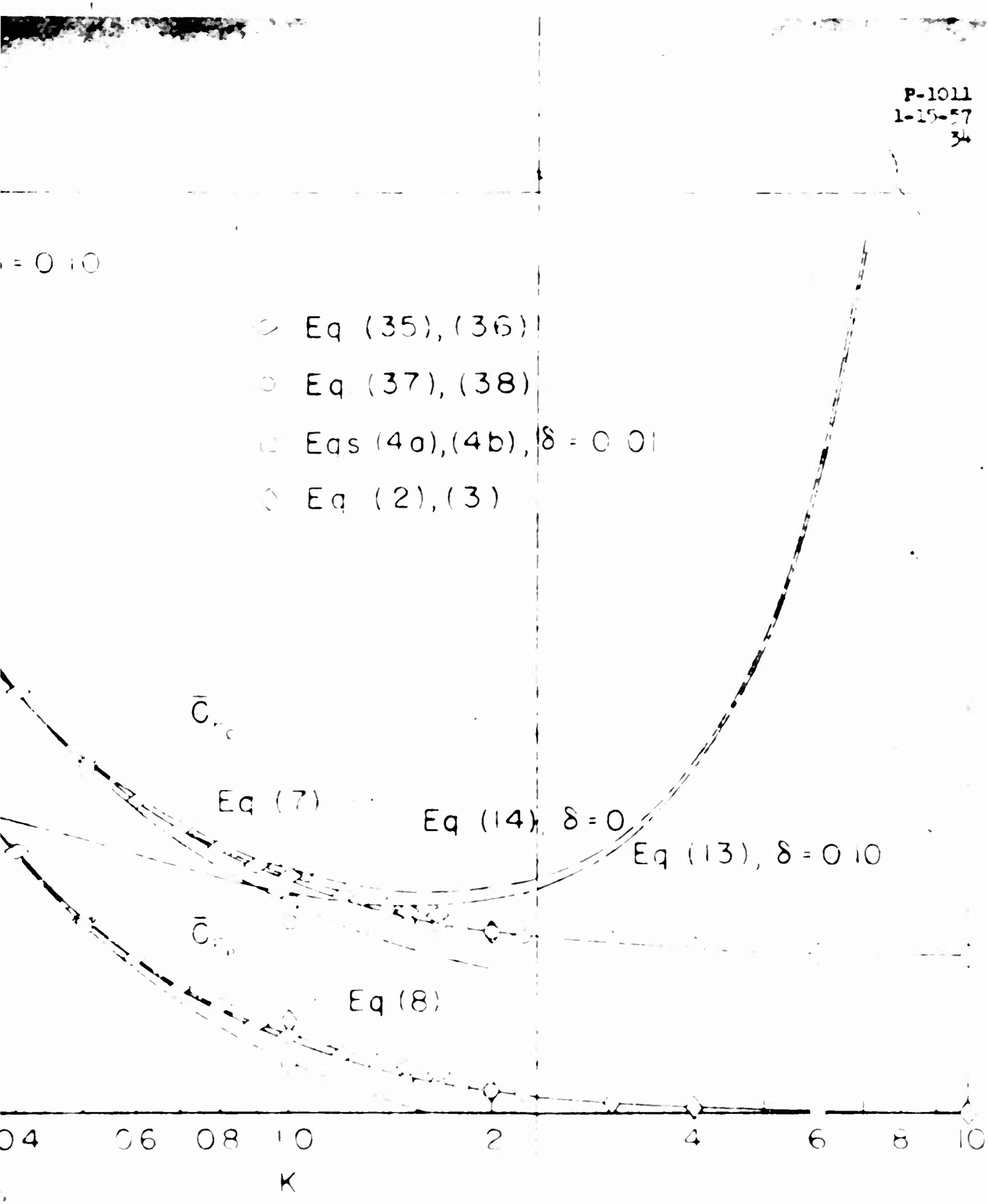

— Two-dimensional pressure coefficients

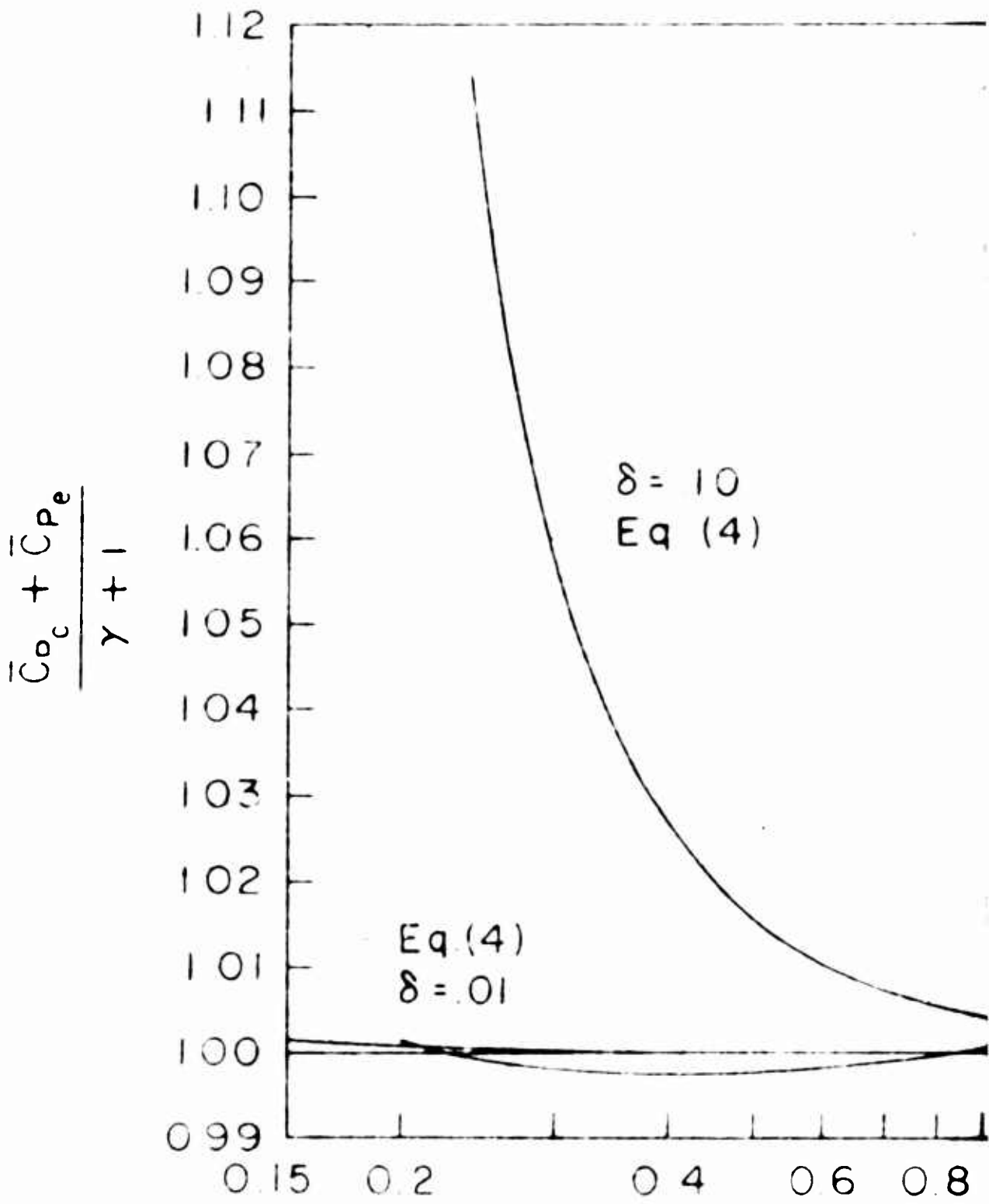

Fig 2 — The normalized sum

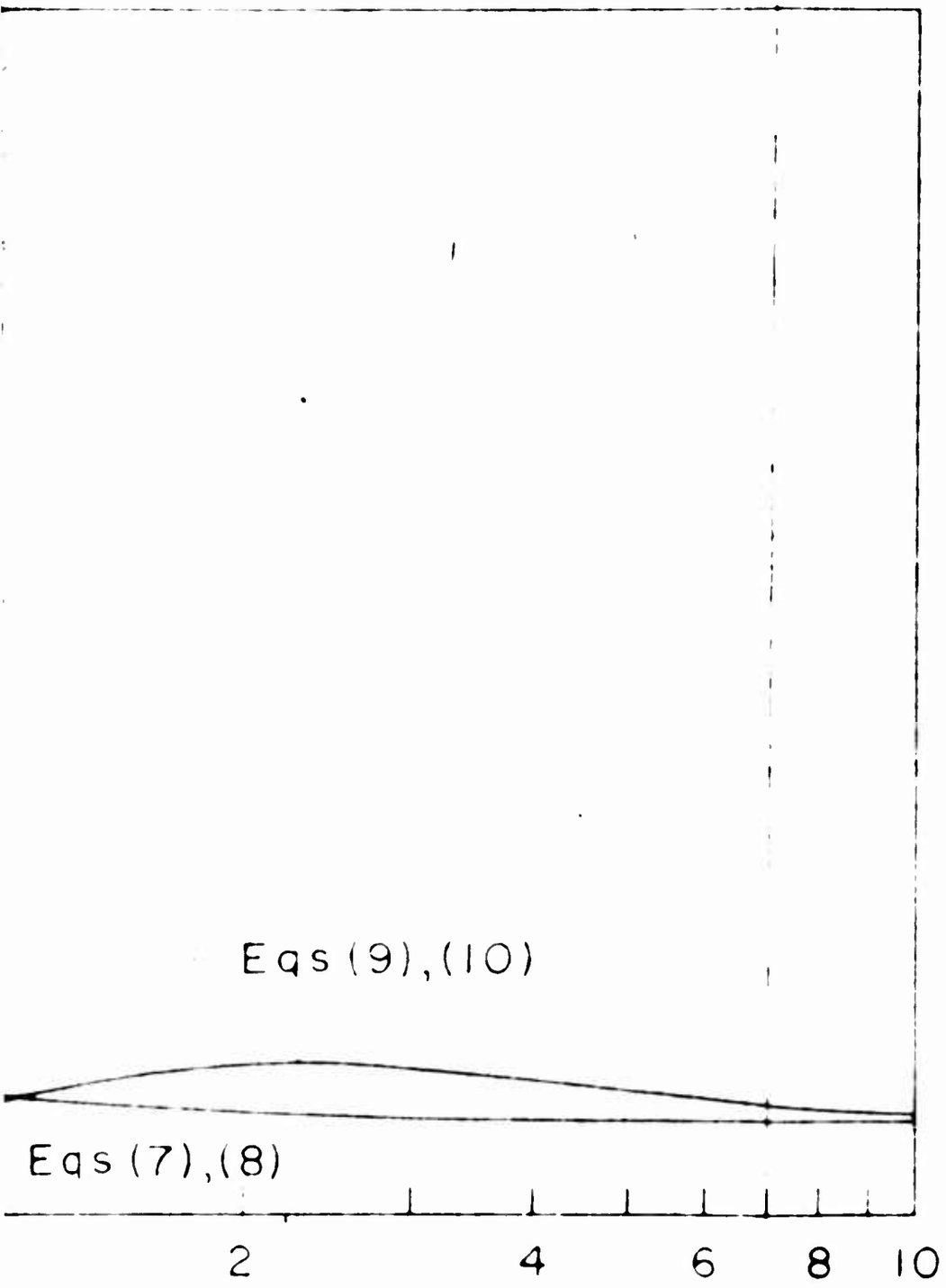

wo-dimensional pressure coefficients

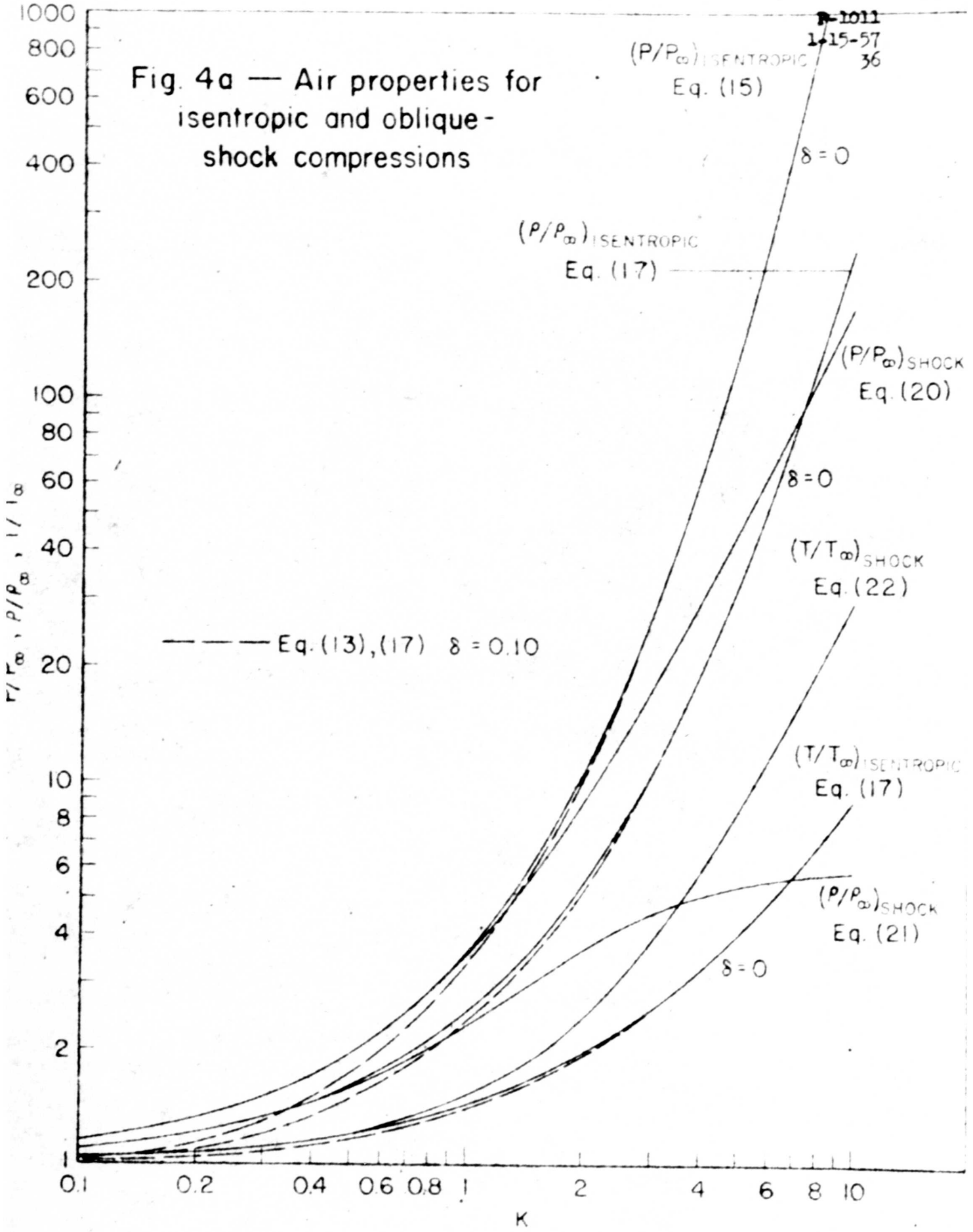
Fig. 4a — Air properties for isentropic and oblique-shock compressions
$(P/P_\infty)_{ISENTROPIC}$ Eq. (15)
δ = 0
$(P/P_\infty)_{ISENTROPIC}$ Eq. (17)
$(P/P_\infty)_{SHOCK}$ Eq. (20)
δ = 0
$(T/T_\infty)_{SHOCK}$ Eq. (22)
Eq. (13), (17) δ = 0.10
$(T/T_\infty)_{ISENTROPIC}$ Eq. (17)
$(P/P_\infty)_{SHOCK}$ Eq. (21)
δ = 0
T/T_∞ , P/P_∞ , I/I_∞
K
1000
800
600
400
200
100
80
60
40
20
10
8
6
4
2
1
0.1
0.2
0.4
0.6
0.8
1
2
4
6
8
10

BLANK PAGE

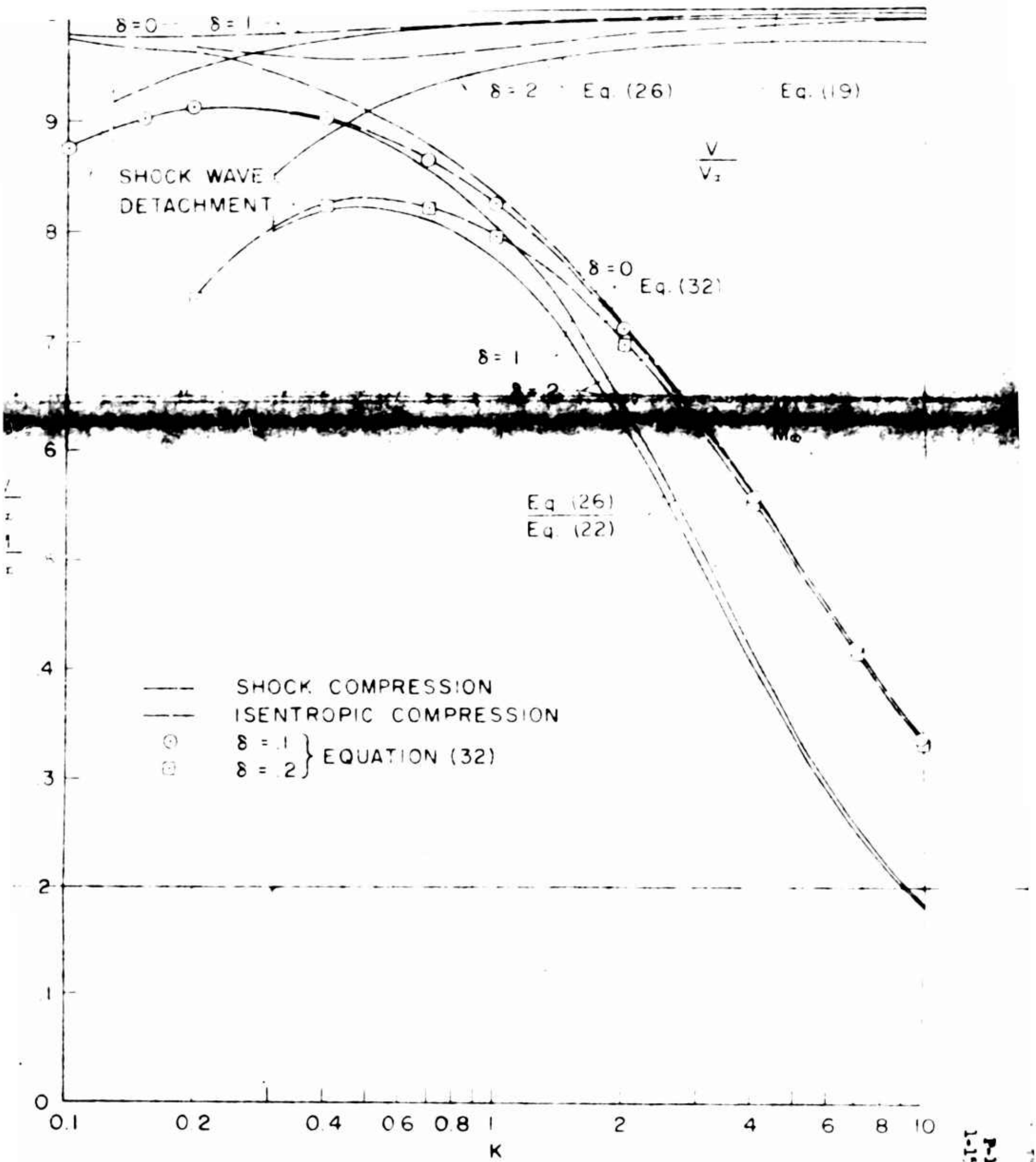

P-1011
1-15-57
47

Fig. 4b — Velocity and mach number for isentropic and oblique-shock compressions

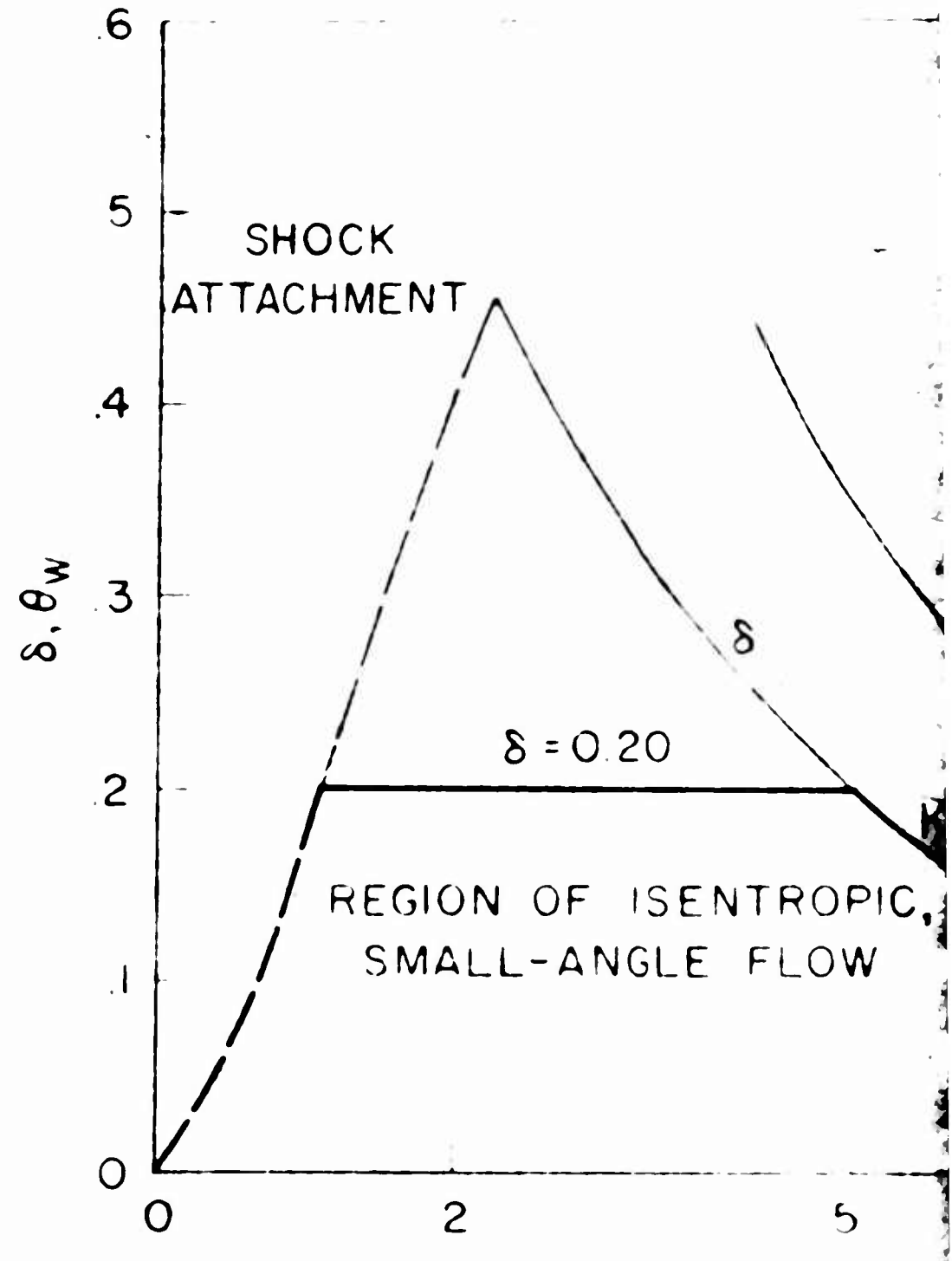

Fig 5 — A re

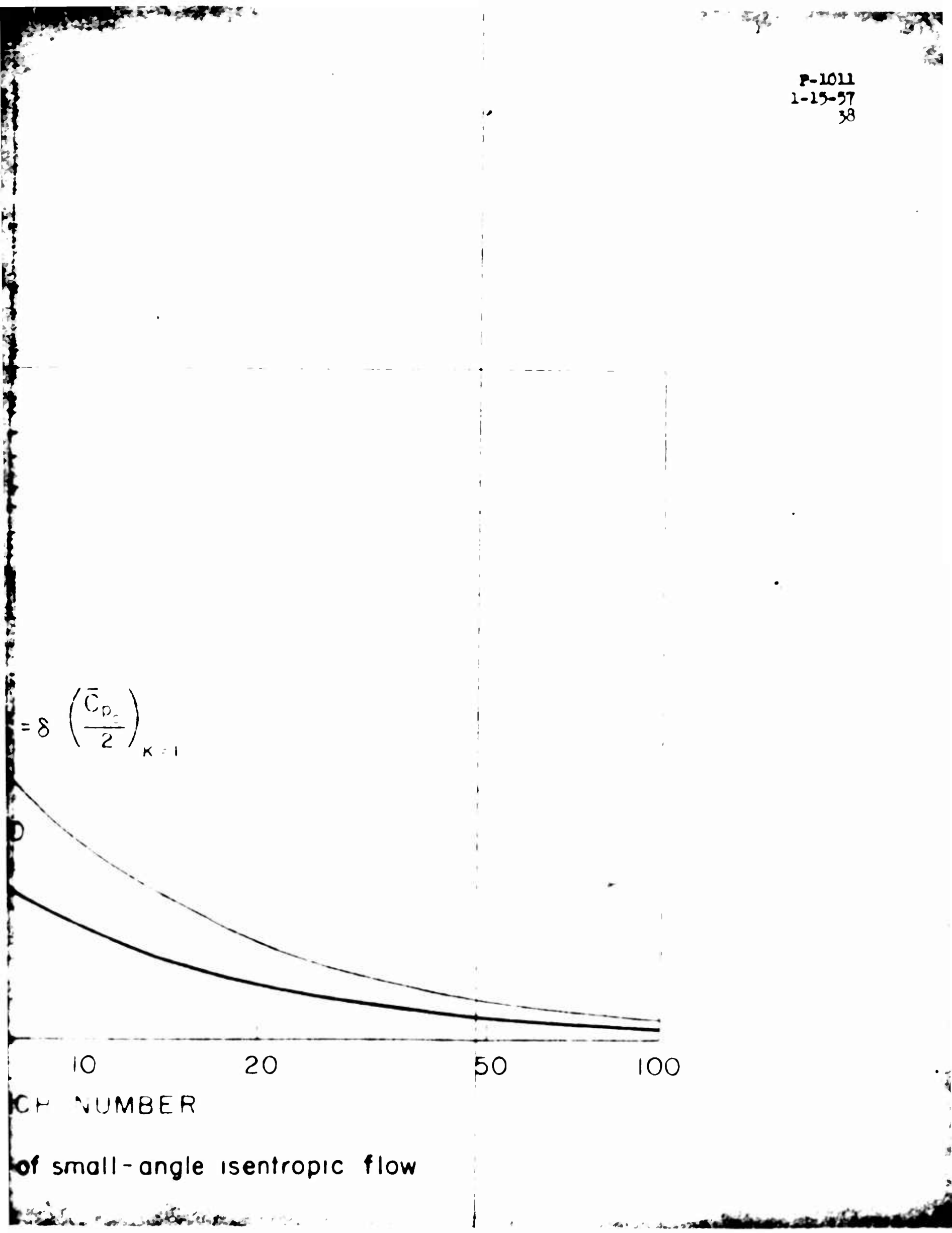

of small-angle isentropic flow

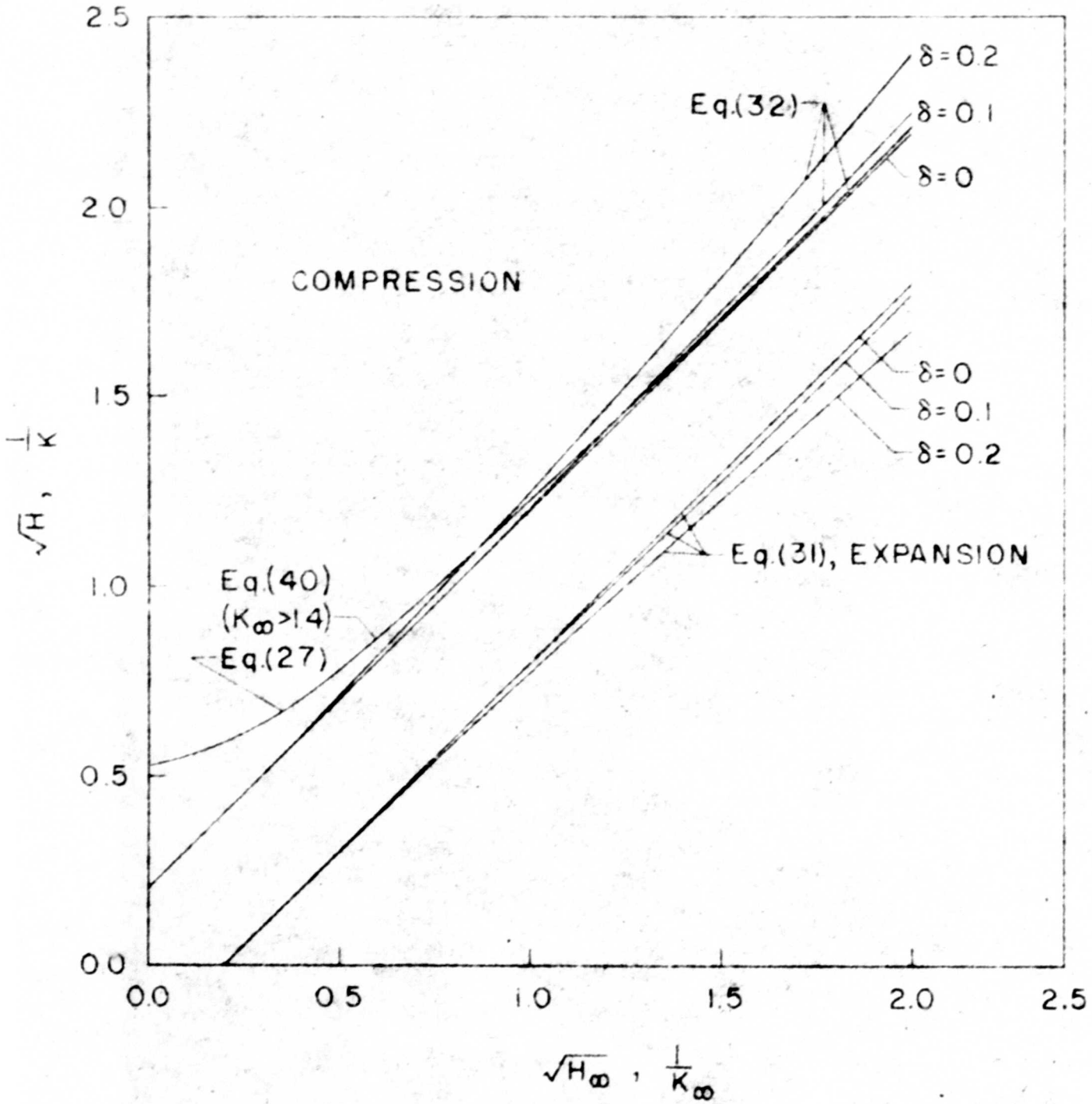

Fig. 6 — The variation of similarity parameter through a compression and an expansion

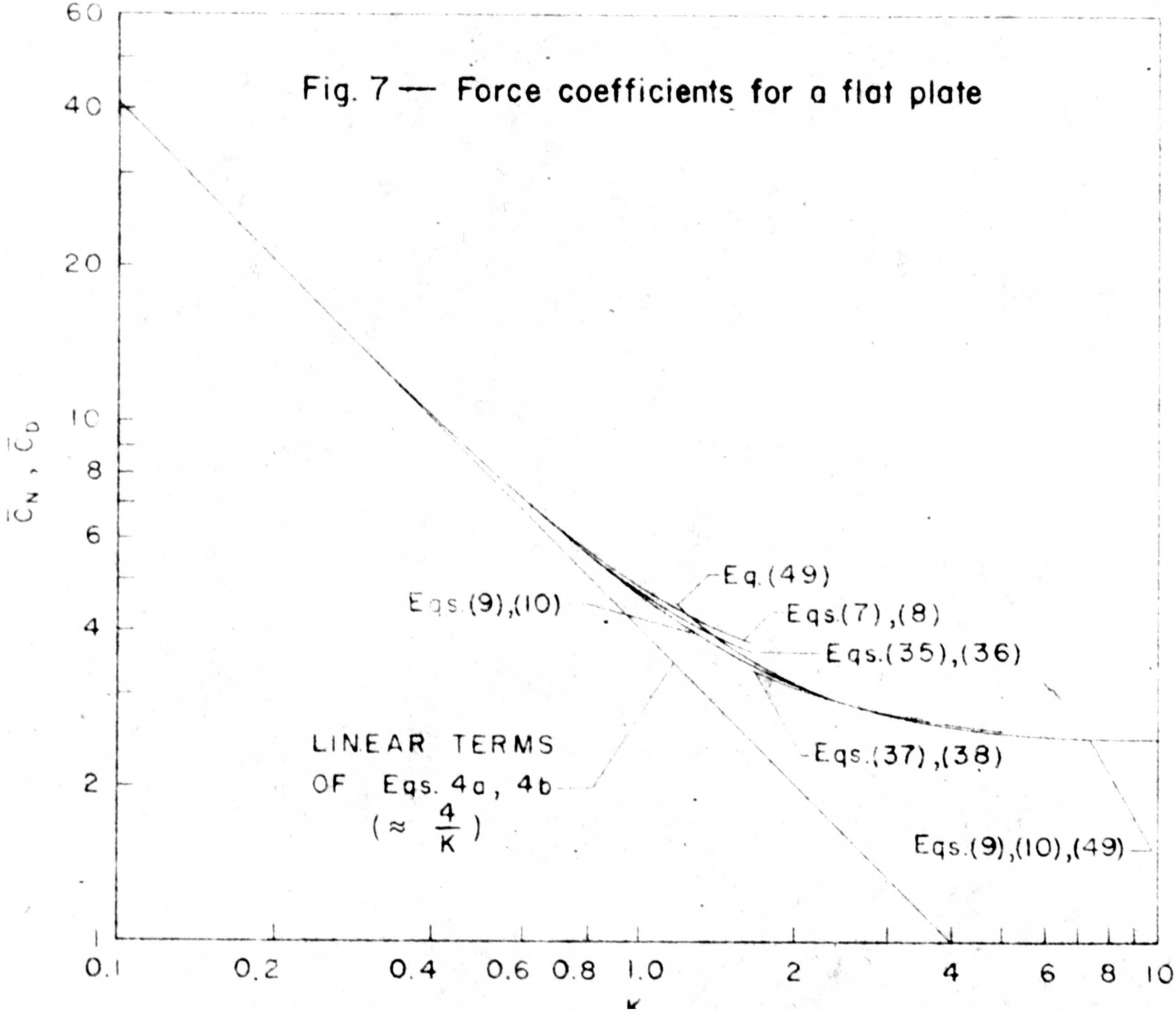

P-1011
1-15-57
ko

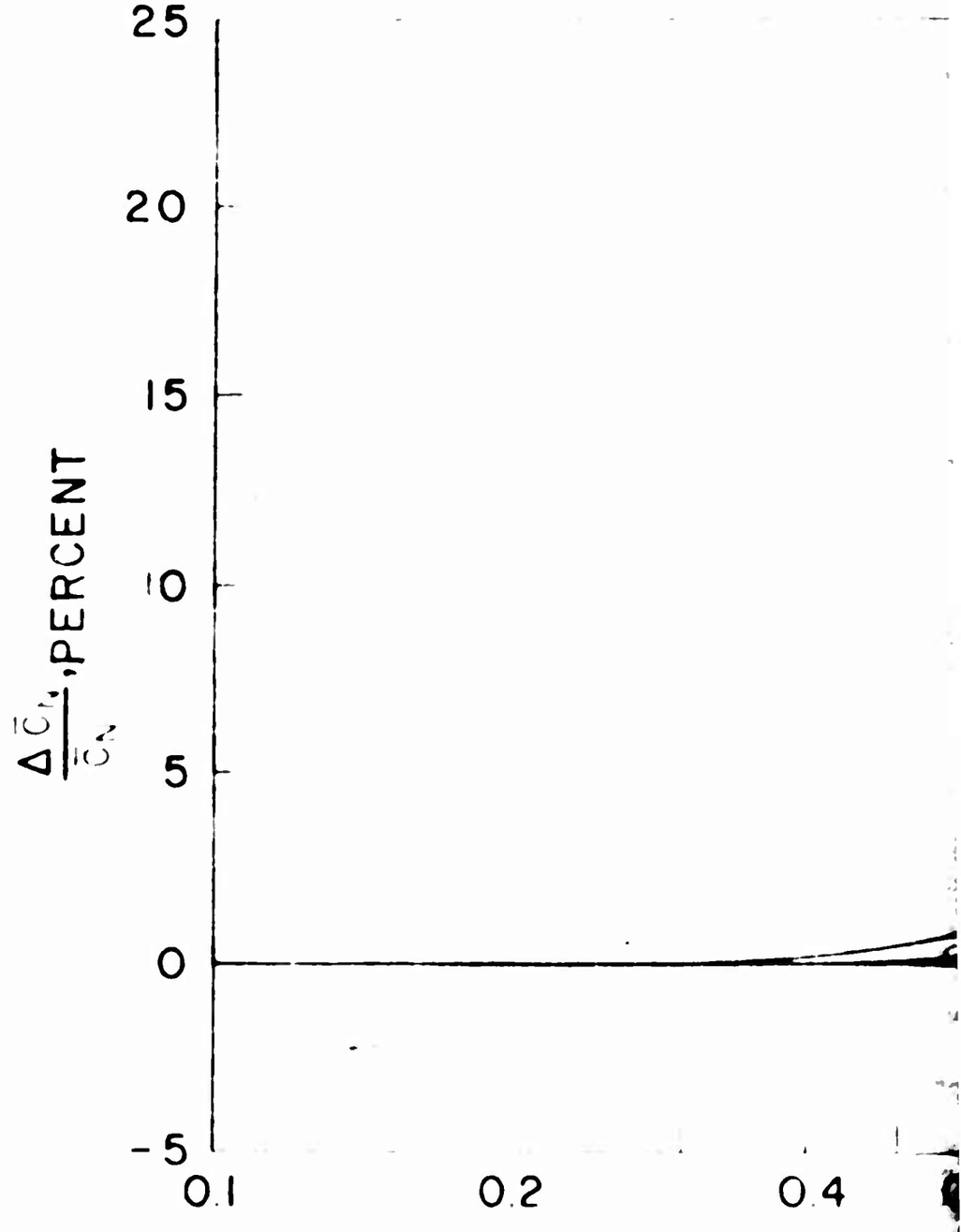

Fig. 8 — A comparis

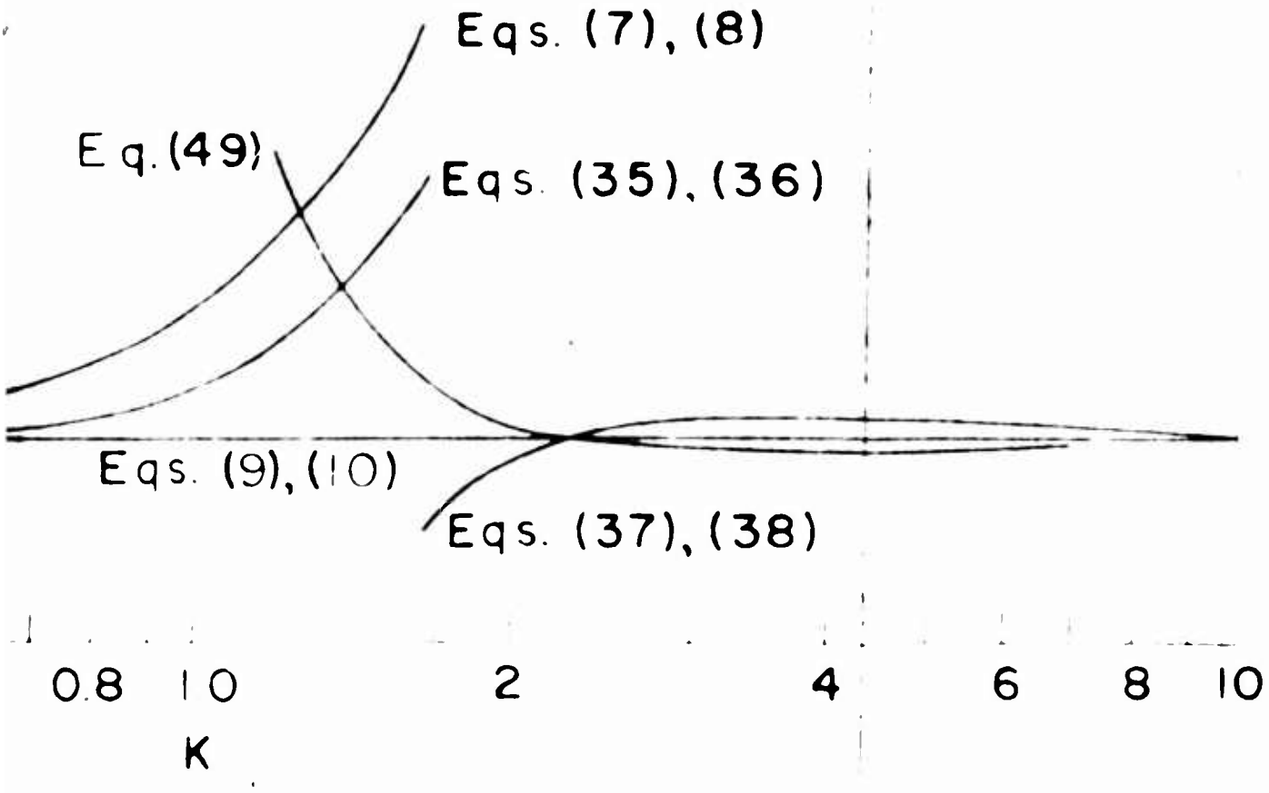

normal force coefficients for a flat plate

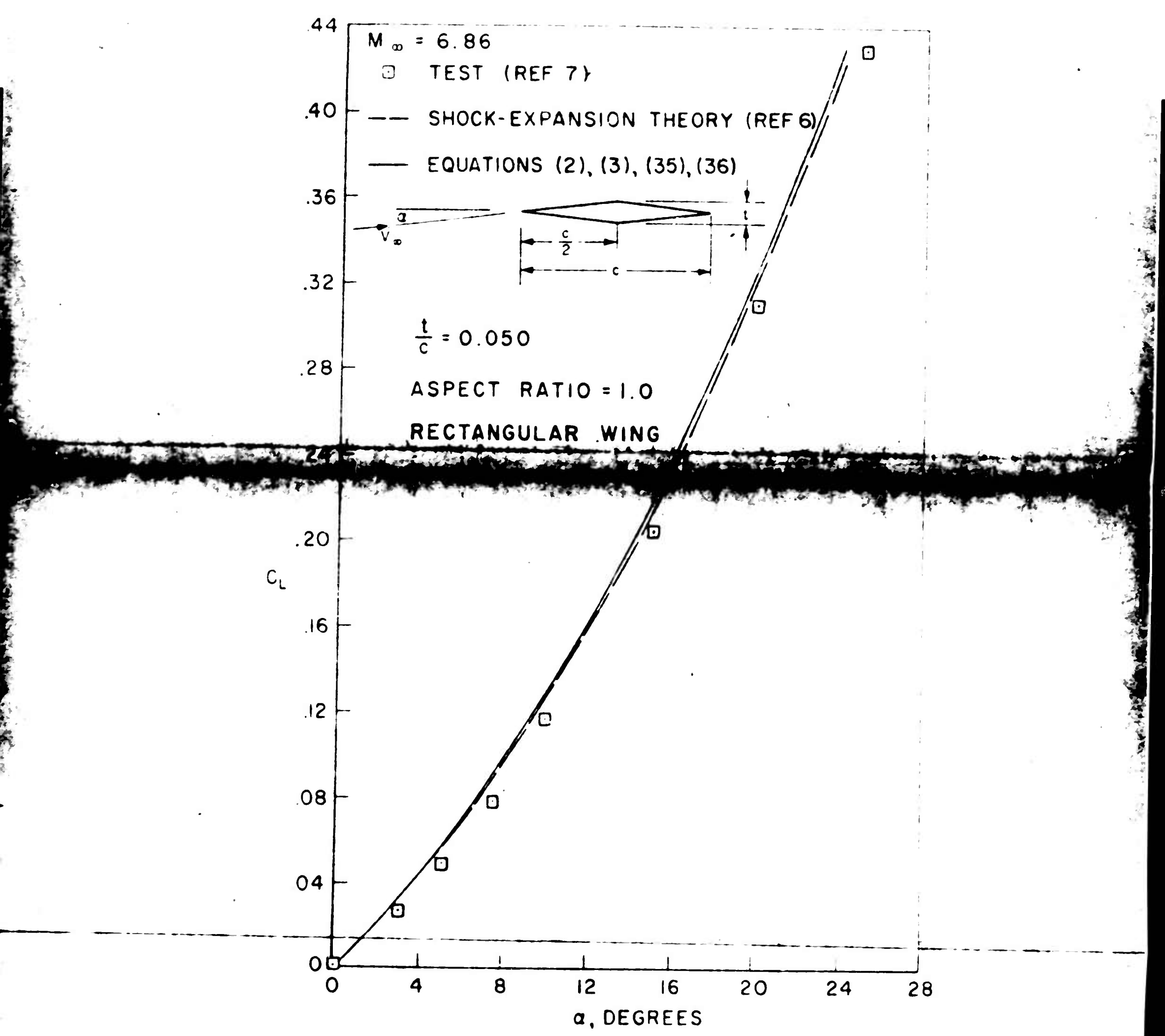

Fig. 10 — A comparison of experimental lift coefficient with theory

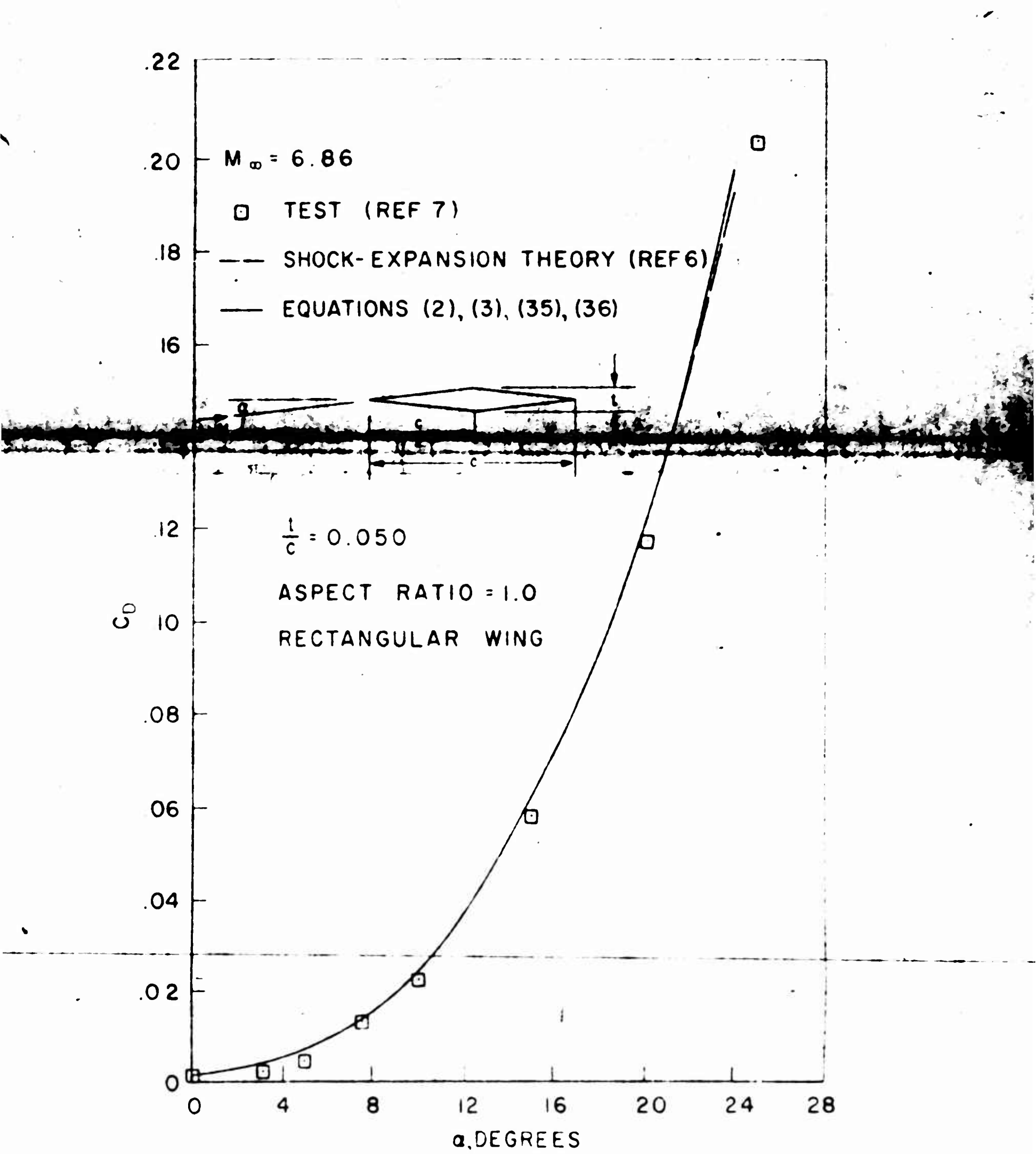

Fig 11 — A comparison of experimental drag coefficient with theory

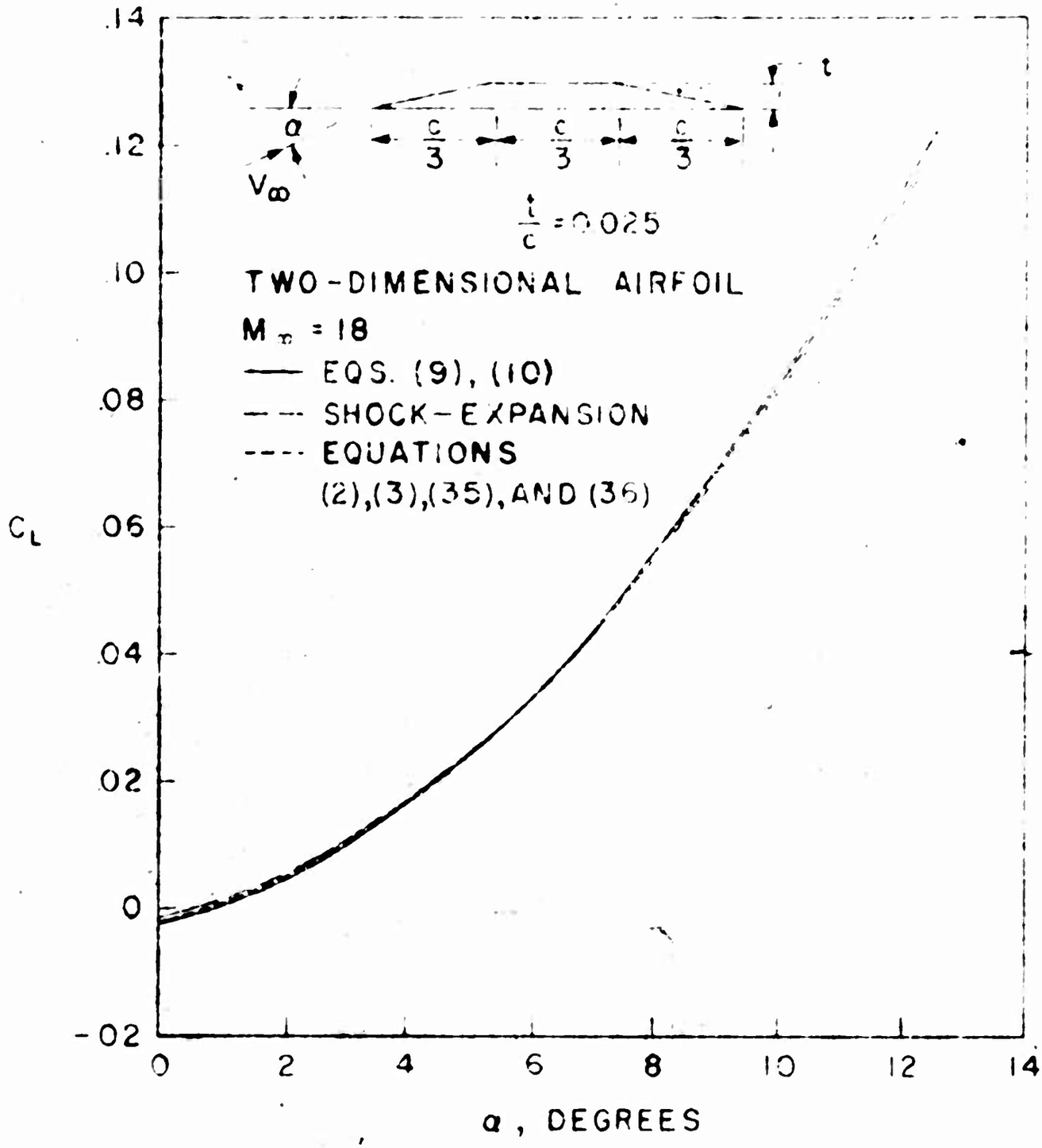

Fig. 12 — Lift coefficient for a modified half-wedge airfoil

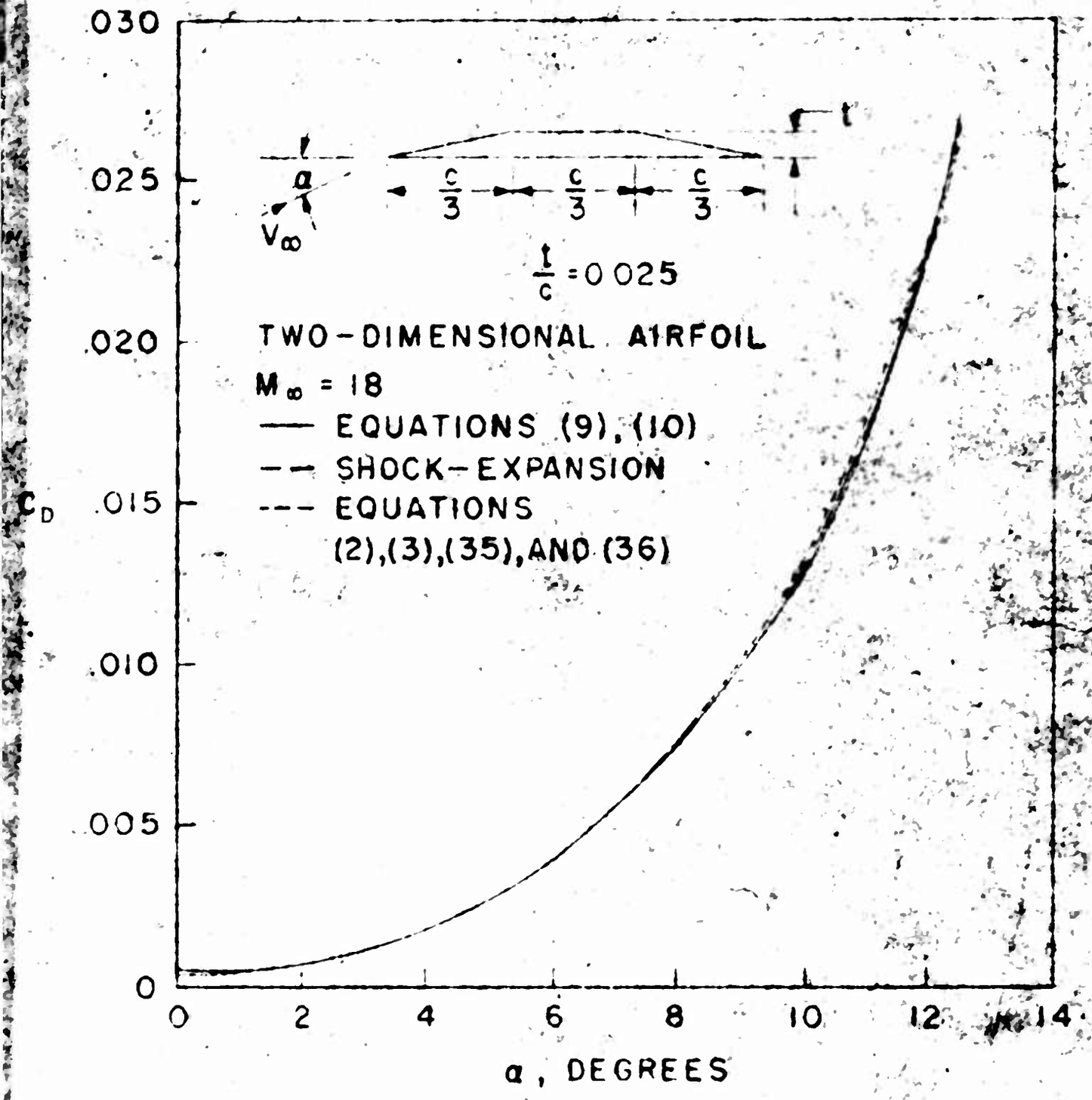

Fig. 13 — Drag coefficient for a modified half-wedge airfoil